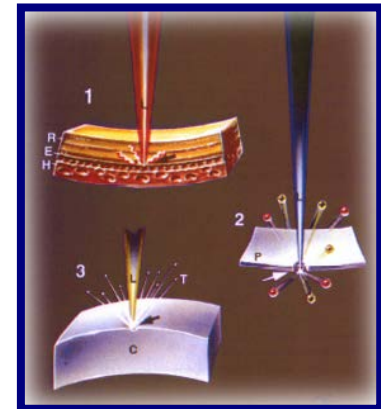
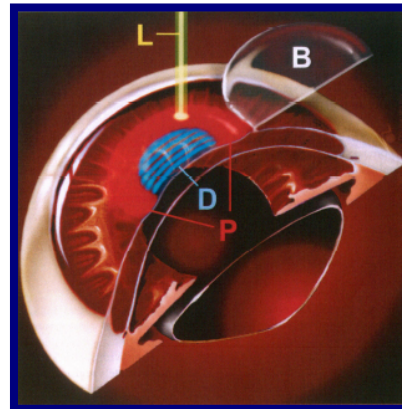
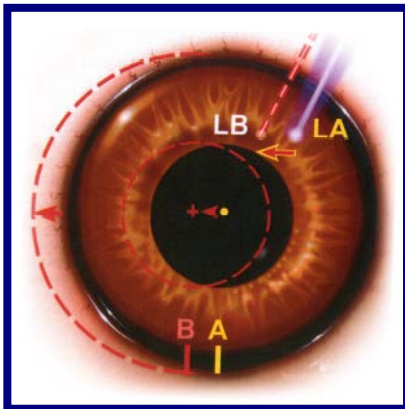
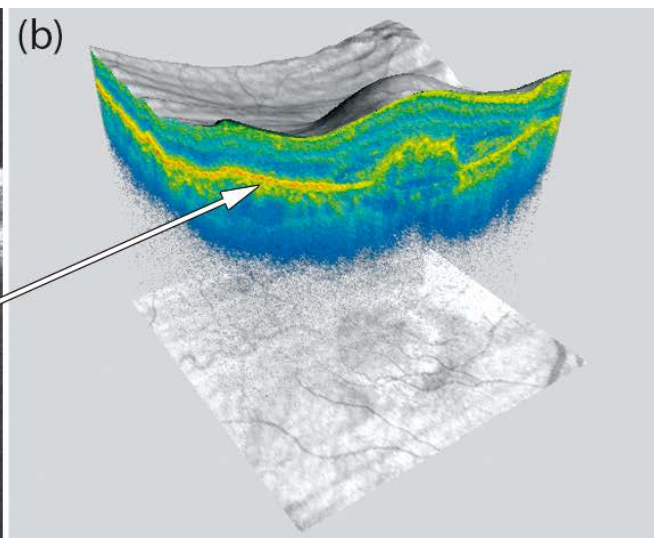
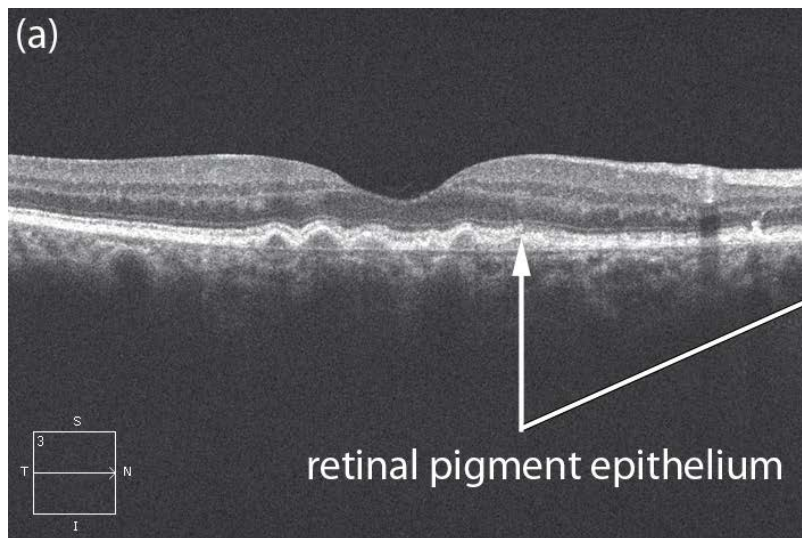


Optical Systems in Medical Technology



Prof. Dr. Michael Kaschke u. Prof. Dr. Werner Nahm
KIT - KSOP | Sommersemester 2018

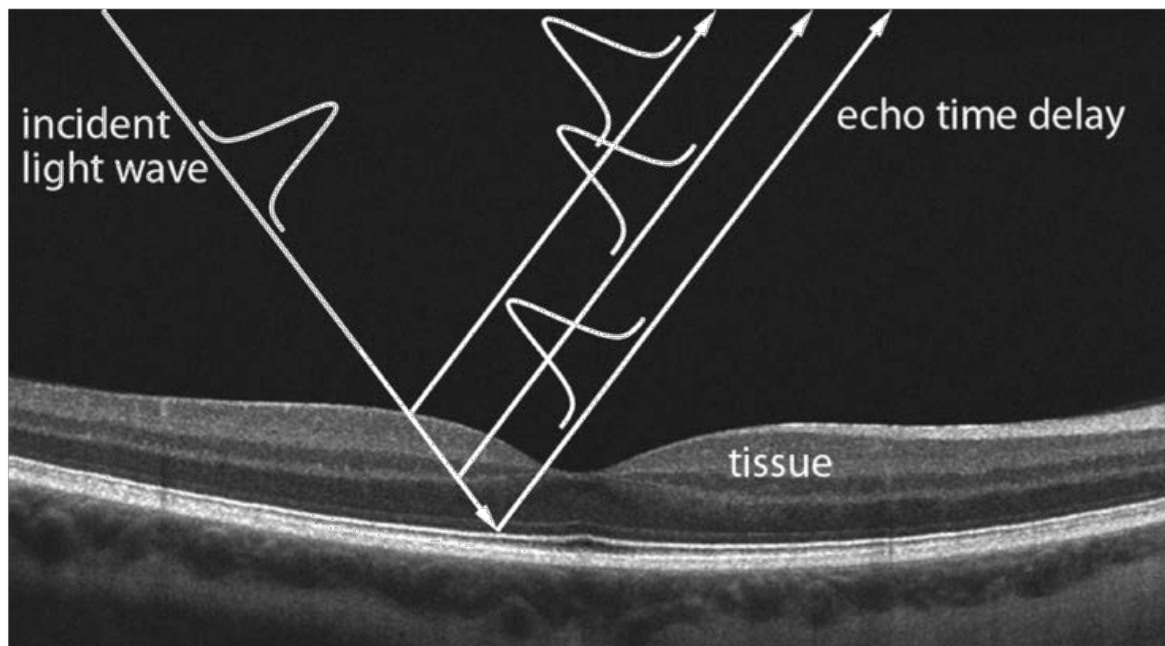
Optical Systems in Medical Technology



Optical Coherence Tomography (OCT)

Introduction OCT = Optical Coherence Tomography

- **Method first shown** in 1991 by Huang et al.
- Low coherence light is used in an interferometer for measuring distances in reflective and backscattering structures
- **Analogy to sonography** = “light acoustic method“

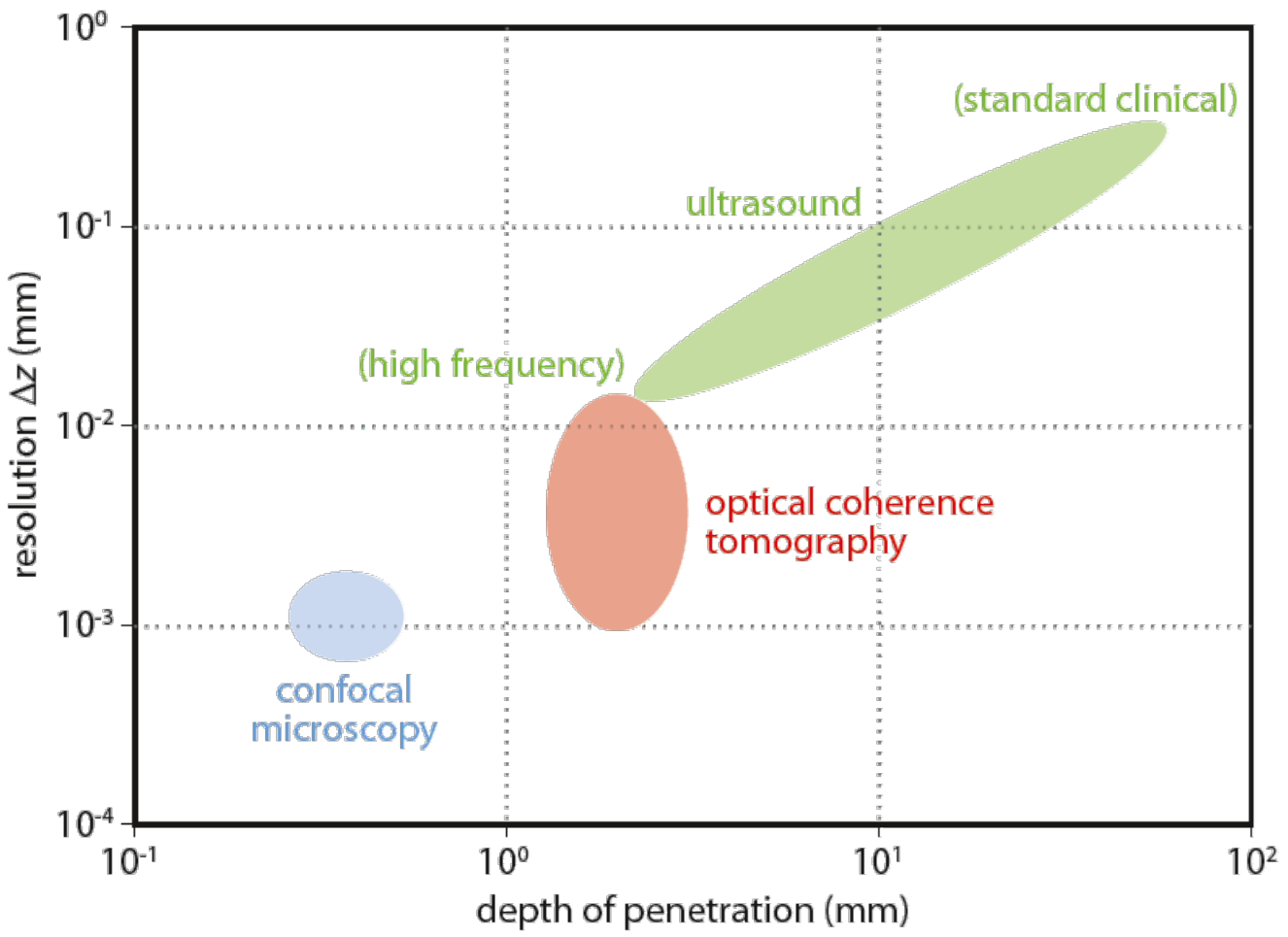


[Science](#). 1991 Nov 22;254(5035):1178-81.

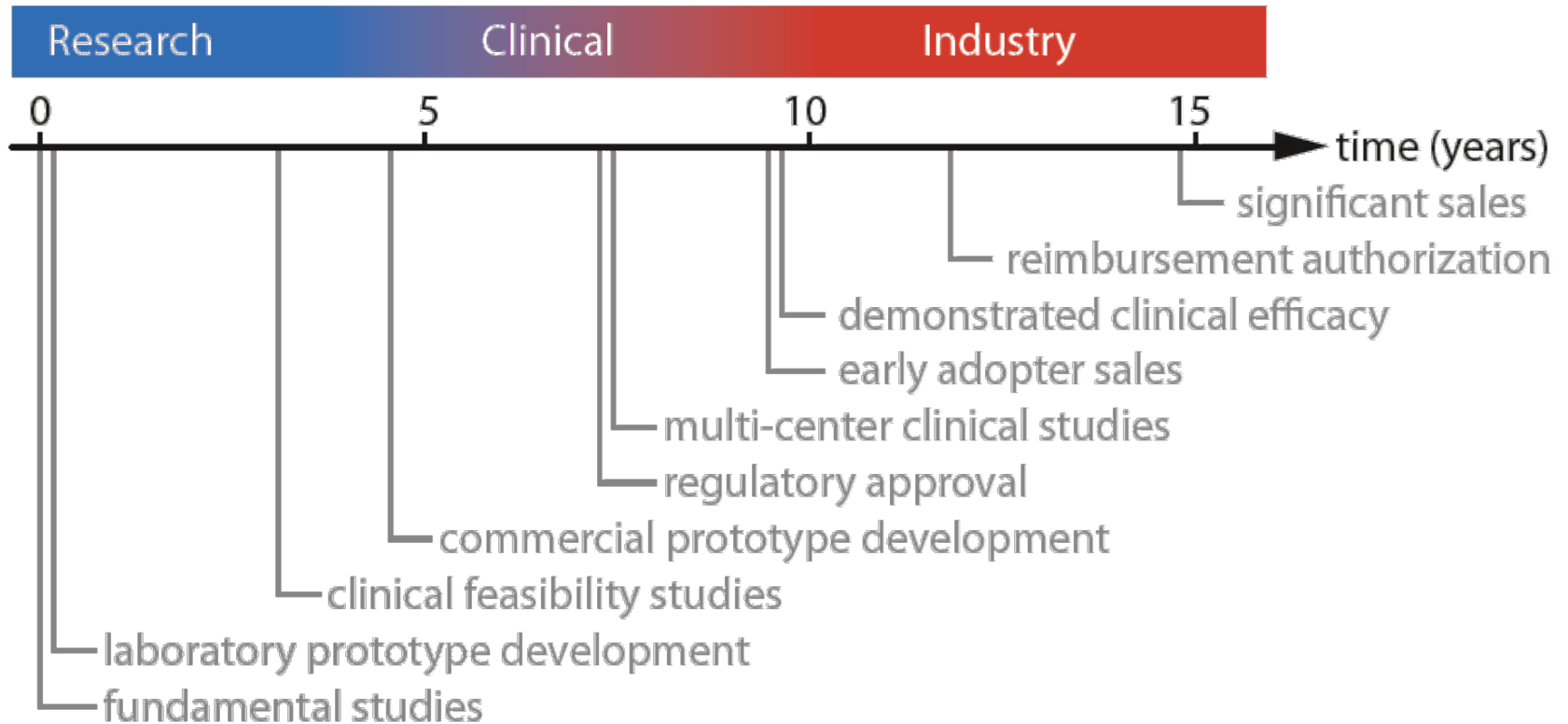
Optical coherence tomography.

[Huang D](#)¹, [Swanson EA](#), [Lin CP](#), [Schuman JS](#), [Stinson WG](#), [Chang W](#), [Hee MR](#), [Flotte T](#), [Gregory K](#), [Puliafito CA](#), et al.

Optical Coherence Tomography (OCT)



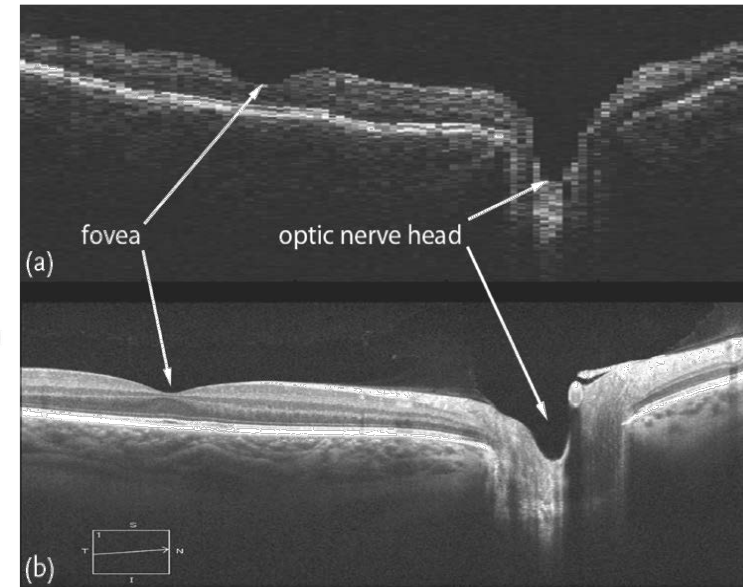
History OCT (Optical Coherence Tomography)



History Optical Coherence Tomography (OCT)

Table 7.1 Milestones of OCT development. Data taken from [12, 21–23].

Year	Milestone
1991	Demonstration of OCT <i>in vitro</i>
1993	First <i>in vivo</i> images of the retina
1994	Carl Zeiss (Humphrey Instruments) acquired OCT technology
1995	Clinical studies with first prototypes
1996	First commercial TD-OCT system introduced (ZEISS OCT 1)
1999	Approximately 200 units sold
2000	Improved commercial system ZEISS OCT 2
2001	Approximately 400 units sold
2002	Second generation TD-OCT system introduced (ZEISS Stratus OCT™)
2005	OCT becomes a standard of care
2006	Approximately 6000 units of ZEISS Stratus OCT sold
2006	Multiple companies enter ophthalmic market with FD-OCT devices
2009	Worldwide OCT revenues exceed US\$ 250 million
2010	US Medicare reimbursed OCT procedures exceed 8 million
2010	Worldwide reimbursement payments exceed US\$ 1 billion
2012	ZEISS Cirrus™ HD-OCT reaches 10 000 installations
2012	Inventors of OCT receive Antonio Champalimaud Vision Award



Basics OCT (I) : Interference of Monochromatic Waves

Superposition of monochromatic waves (incoherent):

$$I_{incoh}(\vec{r}, t) = c \frac{\epsilon_0}{2} [E_1(\vec{r}, t) + E_2(\vec{r}, t)]^2 = I_1(\vec{r}, t) + I_2(\vec{r}, t)$$

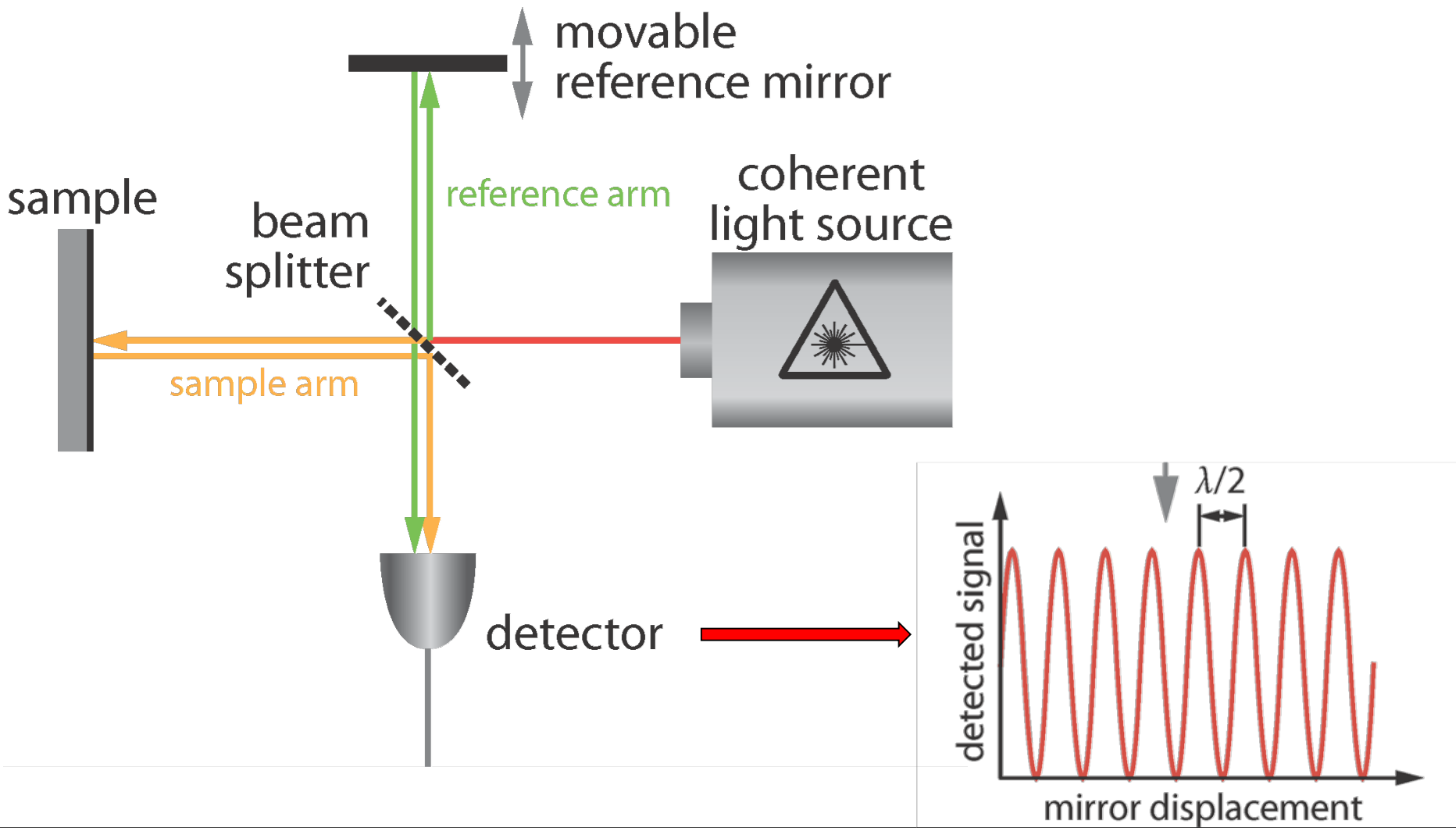
Superposition of monochromatic waves (coherent):

$$I_{coh}(\vec{r}, t) = c \frac{\epsilon_0}{2} [E_1(\vec{r}, t) + E_2(\vec{r}, t)]^2 = I_1(\vec{r}, t) + I_2(\vec{r}, t) + c \frac{\epsilon_0}{2} \text{Re}[E_1(\vec{r}, t)E_2^*(\vec{r}, t)]$$

$$I_{coh}(\vec{r}, t) \propto \left[I_1 + I_2 + \underbrace{2 \cdot E_1 E_2 \cdot \cos(\phi_1(t) - \phi_2(t))}_{\text{Interference Term}} \right]$$

Interference Term

Basics OCT (II) : Michelson – Interferometer (monochromatic)



Basics OCT (III) : Coherence Length, Wiener-Khinchin-Theorem

Coherence Length L_c is the spatial extension across which the electric field is correlated. It is correlated to the **Coherence Time** by:

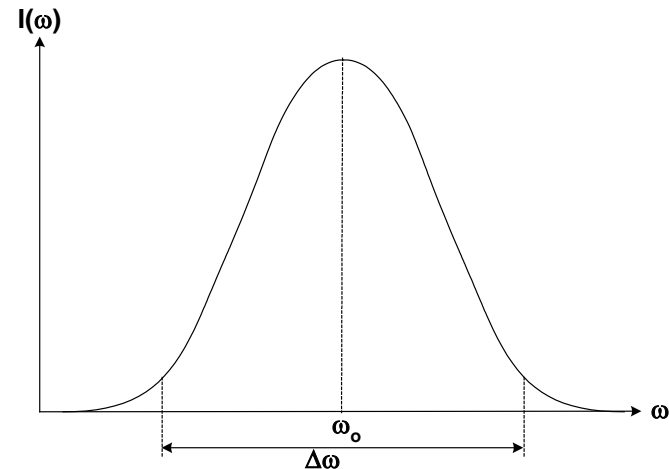
$$L_c = c \cdot \tau_c$$

Light of finite coherence length is called low coherence light and is described by its auto-correlation function:

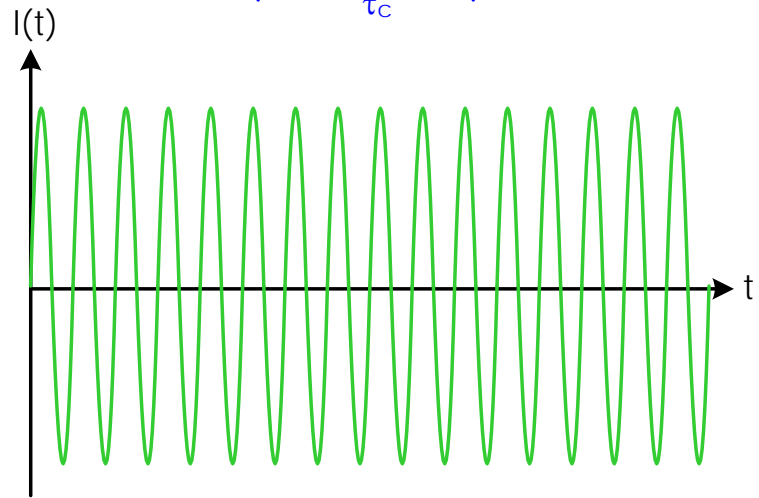
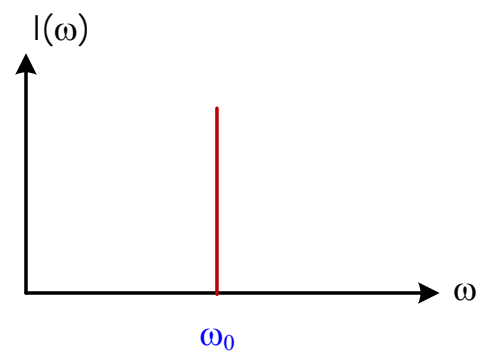
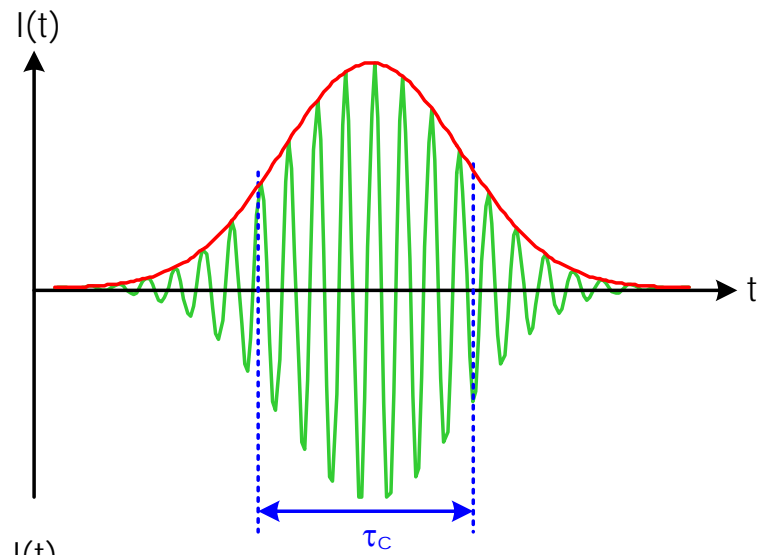
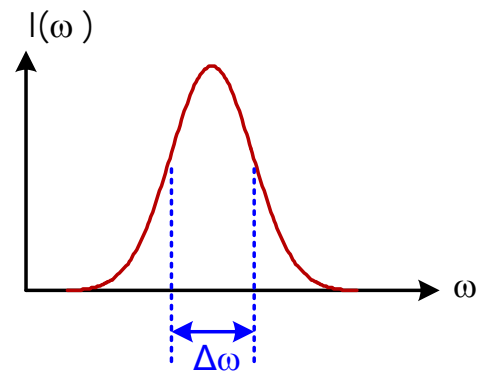
$$G(\tau) = \int_{-\infty}^{+\infty} E(t) \cdot E(t + \tau) dt$$

The Fourier transform of the auto-correlation function is the power spectrum (Wiener-Khinchin-Theorem).

$$I(\omega) = \sigma(\omega) = |E(\omega)|^2 = \int_{-\infty}^{+\infty} G(\tau) e^{i\omega\tau} d\tau$$



Basics OCT (III) : Coherence Length, Wiener-Khinchin-Theorem



Basics OCT (III) : Coherence Length, Wiener-Khinchin-Theorem

Generally

$$L_c = c \cdot \tau_c \approx \frac{2\pi \cdot c}{\Delta\omega}$$

with

$$\Delta\omega = \frac{2\pi \cdot c}{\lambda_0^2} \cdot \Delta\lambda$$

we get

$$L_c \approx \frac{2\pi \cdot c}{\Delta\omega} \approx \frac{\lambda_0^2}{\Delta\lambda}$$

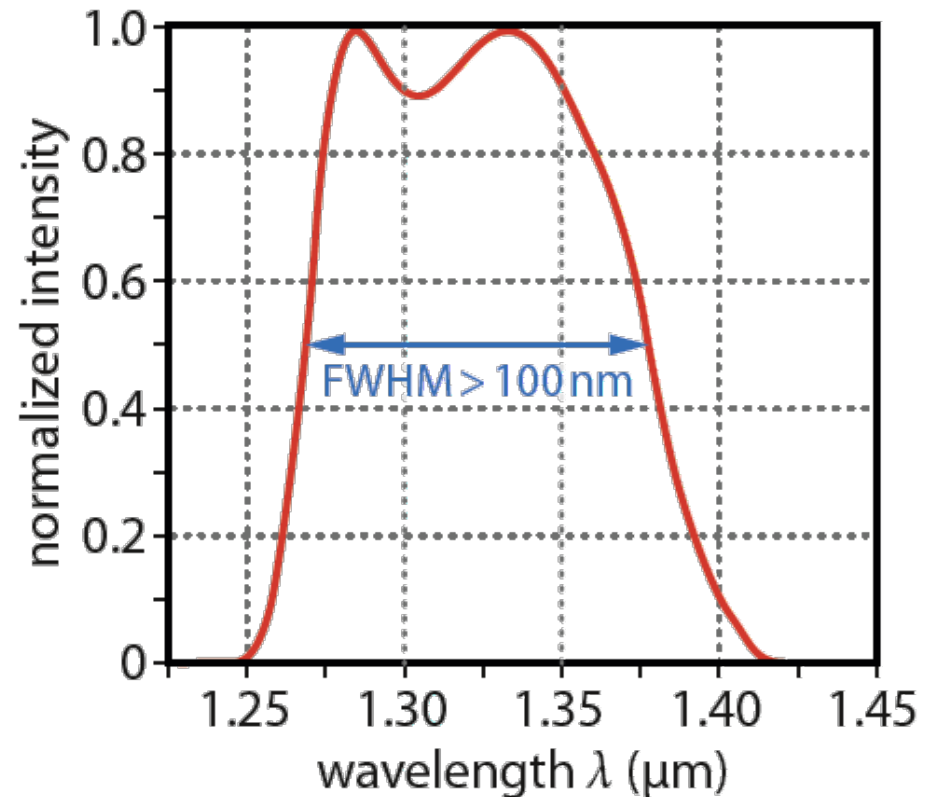
For Gaussian spectrum in particular:

$$L_c = \frac{4 \ln 2}{\pi} \cdot \frac{\lambda_0^2}{\Delta\lambda}$$

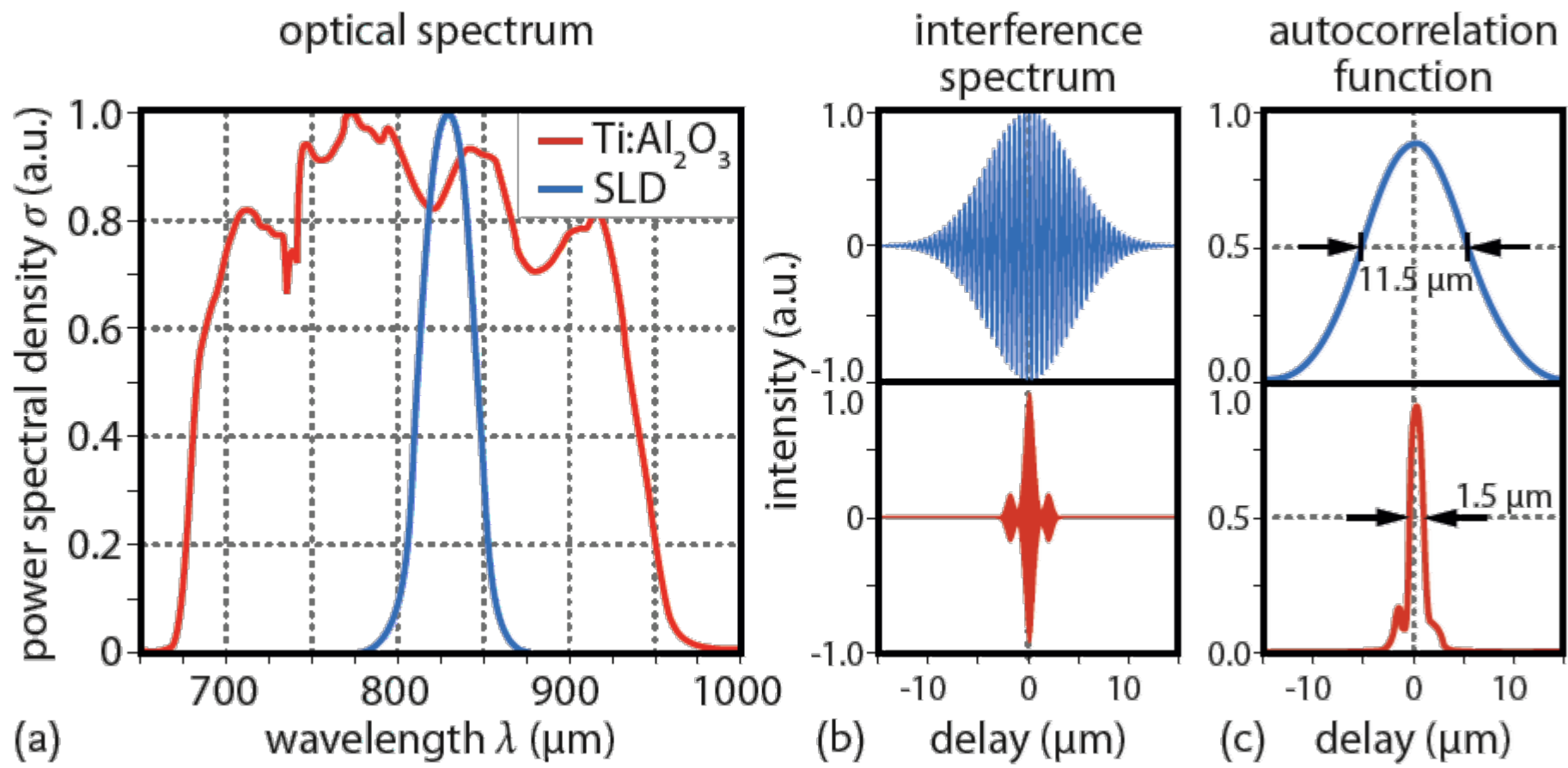
Light Source	τ_c	L_c
Bulb	8.3 fs	2.5 μm
Mercury Lamp	67 fs	20 μm
LED	67 fs	20 μm
Multimode HeNe-Laser	0.67 ns	20 cm
Single Mode HeNe-Laser	1 μs	300 m

OCT- Light Sources– Superluminescence-Diodes

Center wavelength	1325 nm
Bandwidth (FWHM)	> 100 nm
Fiber-coupled power	> 10 mW
Maximum SLD injection current	780 mA
Maximum voltage	4 V
Operating temperature range	0–40 °C



OCT- Light Sources– fs-Ti:Sapphire-Laser



Exercise Coherence Time:

Derive the coherence length of a Gaussian pulse of spectral bandwidth $\Delta\omega$. Express it also in terms of λ_0 and $\Delta\lambda$. Compare this to the pulse duration or the product of pulse duration and speed of light. Use the coherence length of a superluminescence diode (see internet). What differences do you notice?

The intensity of a Gaussian spectrum reads

$$\sigma(\omega) = \sigma_0 \exp \left(-4 \ln(2) \left(\frac{\omega - \omega_0}{\Delta\omega_{\text{FWHM}}} \right)^2 \right) .$$

At the spectral width $\omega = \Delta\omega_{\text{FWHM}}/2 \pm \omega_0$, the intensity is reduced by half of its maximum value. For simplicity, we set $\omega_0 = 0$ and obtain the autocorrelation function as the inverse Fourier transform of the intensity spectrum of the pulse given by

Exercise Coherence Time:

$$\mathcal{G}(\Delta t) = \frac{1}{2\pi} \int_{-\infty}^{+\infty} \sigma_0 \exp \left(-4 \ln(2) \left(\frac{\omega}{\Delta\omega_{\text{FWHM}}} \right)^2 \right) e^{-i\omega\Delta t} d\omega \quad \text{Inverse FT}$$

$$= \frac{1}{2\pi} \int_{-\infty}^{+\infty} \sigma_0 \exp \left(-\frac{4 \ln(2)}{\Delta\omega_{\text{FWHM}}^2} \left(\omega + i \frac{\Delta\omega_{\text{FWHM}}^2 \Delta t}{8 \ln(2)} \right)^2 \right) \cdot \exp \left(-\frac{\Delta\omega_{\text{FWHM}}^2 \Delta t^2}{16 \ln(2)} \right) d\omega \quad \text{Completing the square}$$

$$= \frac{\Delta\omega_{\text{FWHM}}}{4\sqrt{\pi \ln(2)}} S_0 \exp \left(-\frac{\Delta\omega_{\text{FWHM}}^2 \Delta t^2}{16 \ln(2)} \right) \cdot$$

using

$$\int_{-\infty}^{+\infty} e^{-a^2 x^2} dx = \frac{\sqrt{\pi}}{a} \quad \text{with}$$

$$a^2 = \frac{4 \ln(2)}{\Delta\omega_{\text{FWHM}}^2} \cdot$$

Thus, the autocorrelation is again a Gaussian.

Exercise Coherence Time:

Setting $\Delta t = \frac{t_c}{2}$, for the coherence time, at which:

$$\mathcal{G}\left(\frac{t_c}{2}\right) = \frac{1}{2} \mathcal{G}_0 = \frac{1}{2} \left(\frac{\Delta\omega_{\text{FWHM}}}{\sqrt[4]{\pi \ln(2)}} \sigma_0 \right) !$$

The exponential becomes:

$$\begin{aligned} \exp\left(-\frac{\Delta\omega_{\text{FWHM}}^2 t_c^2}{4 \cdot 16 \ln(2)}\right) &= \frac{1}{2} \\ \Rightarrow \frac{\Delta\omega_{\text{FWHM}}^2 t_c^2}{4 \cdot 16 \ln(2)} &= \ln(2) \end{aligned}$$

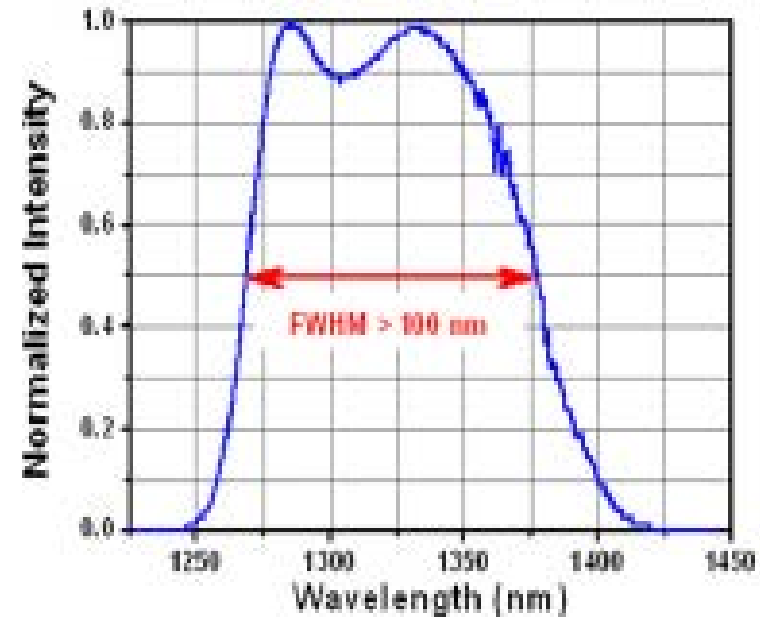
$$\Rightarrow t_c = \frac{8 \ln(2)}{\Delta\omega_{\text{FWHM}}} .$$

With $\omega_0 = 2\pi c/\lambda_0$ and $|\Delta\omega_{\text{FWHM}}| = 2\pi c\lambda_{\text{FWHM}}/\lambda_0^2$, the coherence length thus follows as

$$L_c = ct_c = \frac{8 \ln(2) c}{\Delta\omega_{\text{FWHM}}} = \frac{4 \ln(2)}{\pi} \frac{\lambda_0^2}{\Delta\lambda_{\text{FWHM}}} .$$

Exercise Coherence Time:

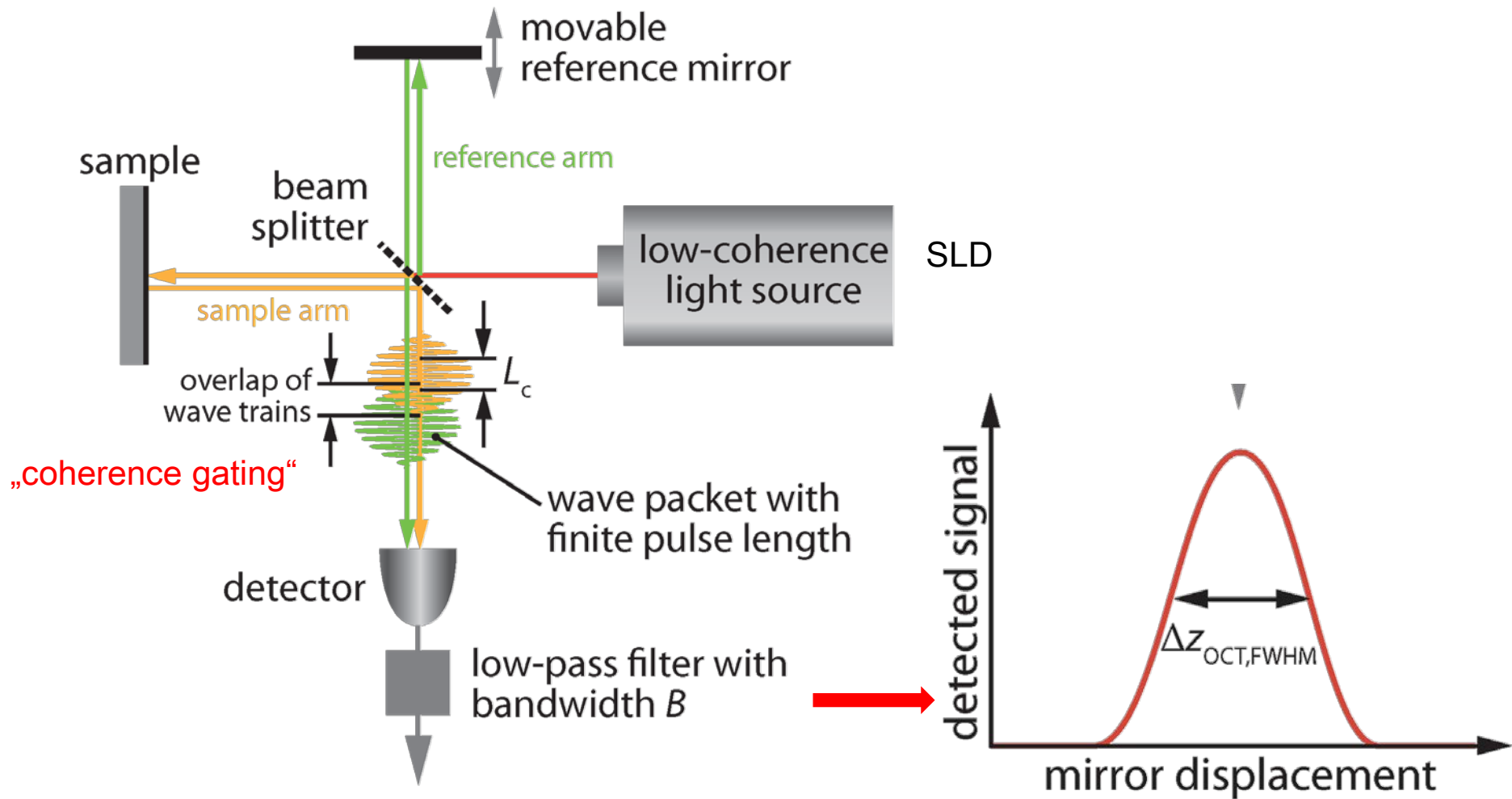
SPECIFICATIONS	
Central Wavelength	1325 nm
Bandwidth (FWHM)	>100 nm
Fiber-Coupled Power	>10 mW
LED Injection Current (Max)	700 mA
Voltage (Max)	4 V
Operating Temperature Range	0 – 40 °C
Isolation of Integrated Isolator	>30 dB
Fiber Signal	SMD-20+
Fiber Length	~1 m
Fiber Connector	FC/APC
Return Loss of FC/APC Connector	>50 dB
Thermoelectric Cooler Current (Max)	4 A
Thermoelectric Cooler Voltage (Max)	4 V
Thermal Resistance*	10 K/W



$$\lambda_0 = 1325 \text{ nm and } \Delta\lambda_{\text{FWHM}} = 100 \text{ nm}$$

$$L_c = ct_c = \frac{4 \ln(2)}{\pi} \frac{\lambda_0^2}{\Delta\lambda_{\text{FWHM}}} = 16 \mu\text{m}$$

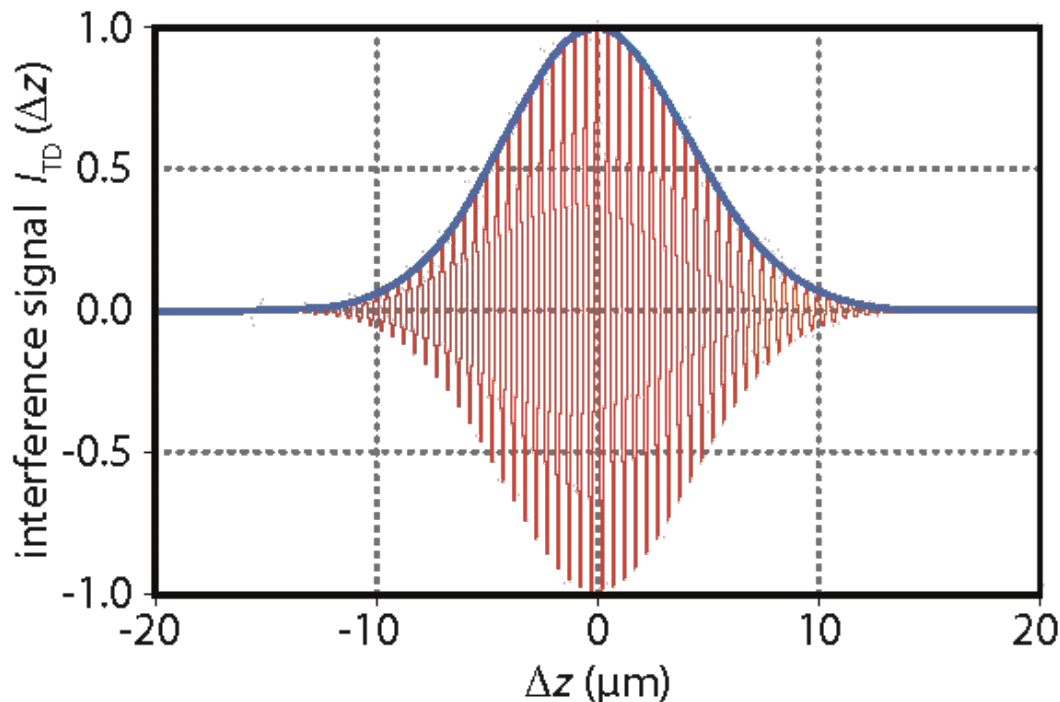
Time-Domain OCT - Michelson – Interferometer (low coherence light)



Time-Domain OCT - Axial Resolution

Axial resolution Δz_A is FWHM (Full Width Half Maximum Gaussian) of the envelope of the detector's AC-signal.

$$\Delta z_{\text{OCT,FWHM}} = \frac{2 \ln(2)}{\pi} \frac{\lambda_0^2}{\Delta \lambda} \quad \text{or with} \quad L_c = \frac{4 \ln(2)}{\pi} \frac{\lambda_0^2}{\Delta \lambda} \quad \text{we have} \quad \Delta z_{\text{OCT,FWHM}} = L_c / 2$$



Axial Resolution of TD-OCT is half the coherence length of the light source (in air)

In matter with refractive index n we have:

$$\Delta z_{\text{OCT,FWHM}} = L_c / 2n$$

OCT – Advantage: Independent Lateral and Axial Resolution

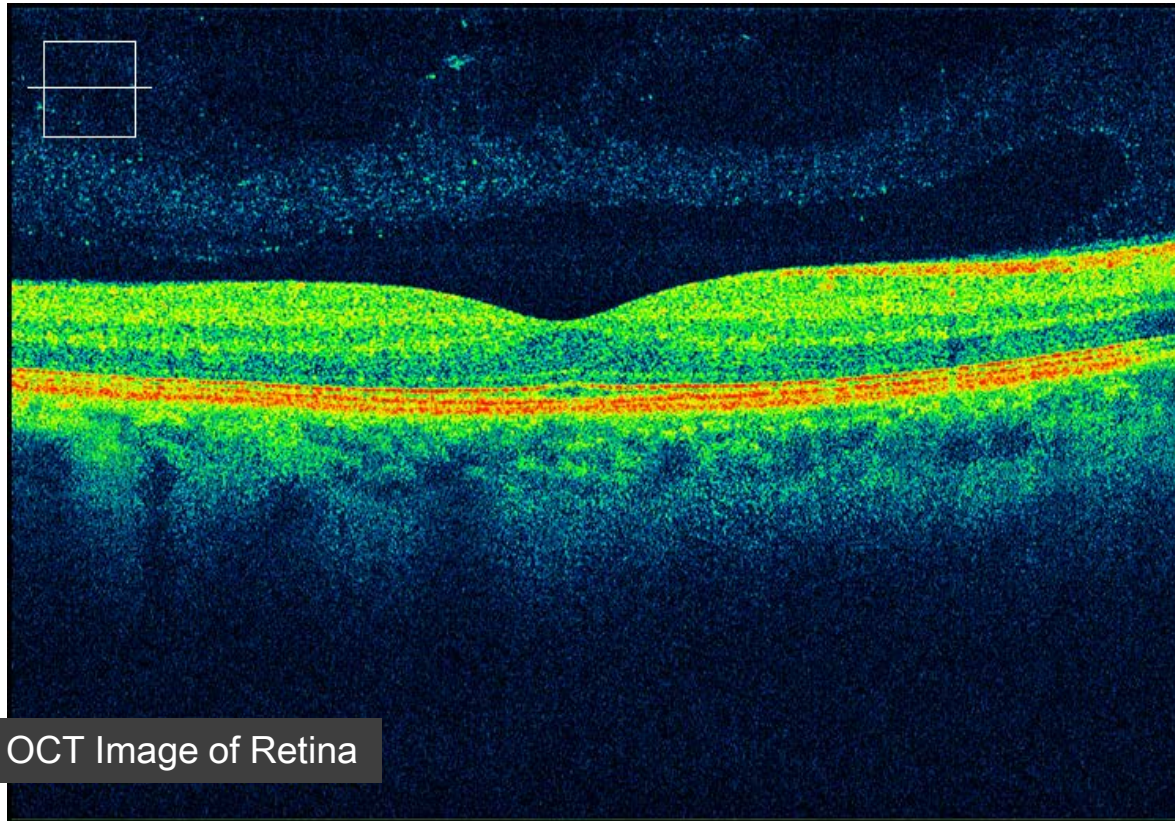
- In contrast to standard microscopy lateral (transverse) and axial resolution are **decoupled**. This is one of the **key advantages of OCT**.
- In OCT, the axial resolution does not depend on the numerical aperture NA, but only on the **coherence length** of the used light.

	OCT	Microscope
Lateral resolution $\Delta x, y$	$\Delta x, y \sim \lambda/NA$	$\Delta x, y \sim \lambda/NA$
Axial resolution Δz	$\Delta z \sim L_c/2$	$\Delta z \sim \lambda/NA^2$

Example:

- $NA_{\text{Eye}} = \frac{d_{\text{Pupil}}}{2 s_{\text{nv}}} = \frac{4 \text{ mm}}{250 \text{ mm}} = 0.016$ and $\lambda = 850 \text{ nm}$
- Thus, we have for normal microscopy: $\Delta x \approx 50 \mu\text{m}$ $\Delta z \approx 350 \mu\text{m}$
- In contrast for OCT: $\Delta x \approx 50 \mu\text{m}$ $\Delta z \approx 8 \mu\text{m}$

Lateral (Transverse) and Axial Resolution



OCT Image of Retina

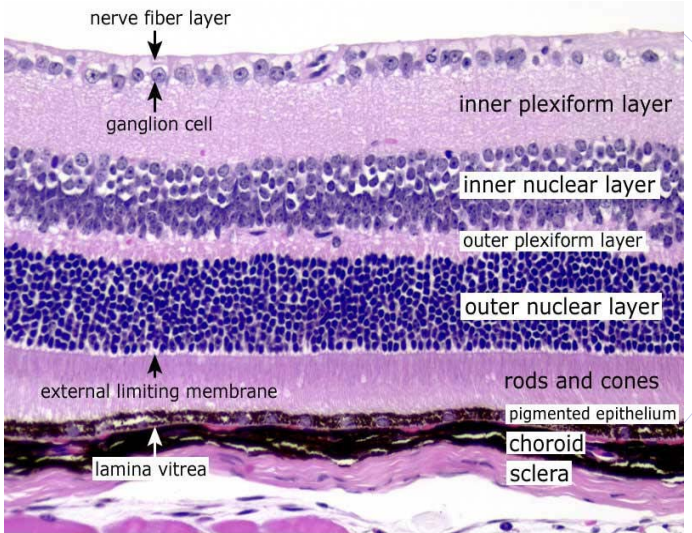
Axial resolution determines which layers in z-direction can be distinguished/resolved.

The axial resolution is determined by the characteristics of the light source.

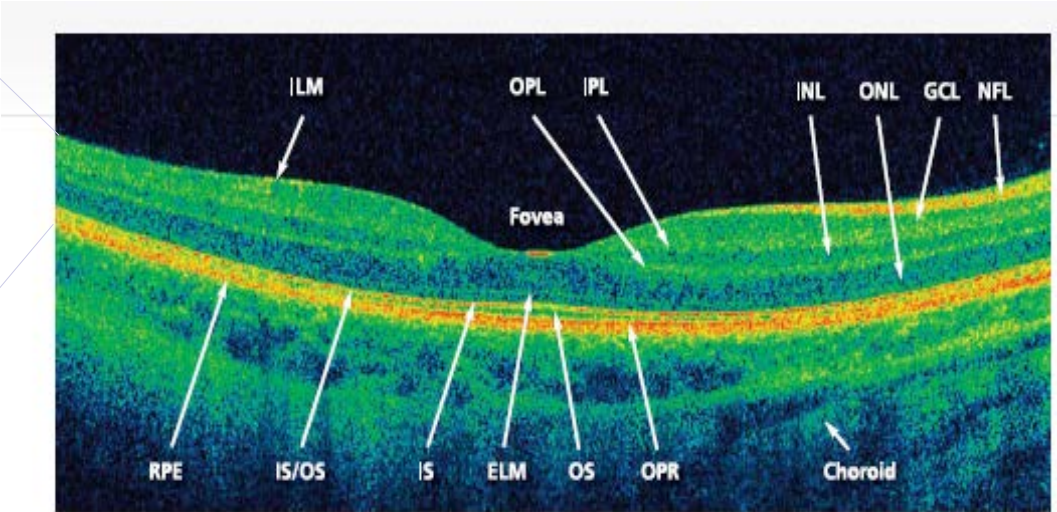
The transverse resolution is limited by the numerical aperture of the entire optical system, i.e. measuring system and sample. In ophthalmology the pupil diameter and the NA of the scanner determine the resolution limit.

Reflectivity of Eye at 800 nm to 1100 nm provides reasonable contrast in the retina

OCT has become a Standard Scanning Imaging Method in Ophthalmology



© Deltagen Inc.



- | | | |
|------------------------------|---------------------------------|--------------------------------------|
| NFL: Nerve fiber layer | OPL: Outer plexiform layer | IS/OS: Interface between IS and OS |
| ILM: Inner limiting membrane | ONL: Outer nuclear layer | RPE: Retinal pigment epithelium |
| GCL: Ganglion cell layer | ELM: External limiting membrane | OPR: Outer photoreceptor/RPE complex |
| IPL: Inner plexiform layer | IS: Photoreceptor inner segment | |
| INL: Inner nuclear layer | OS: Photoreceptor outer segment | |

Evolution of TD-OCT to OCT in the Frequency Domain (FD-OCT)

TD-OCT:

- Low coherent light with center wavelength λ_0 is used in an interferometer in which one arm contains the sample
- An interference signal is measured exactly then when reference and sample path lengths match within the coherence length
- Backscattering information from a particular sample layer are obtained by scanning the reference path length.
- For this backscattering interference signal at every time of the scan t we have: $L_{probe} = L_{ref}$.

Basic principle for evolution:

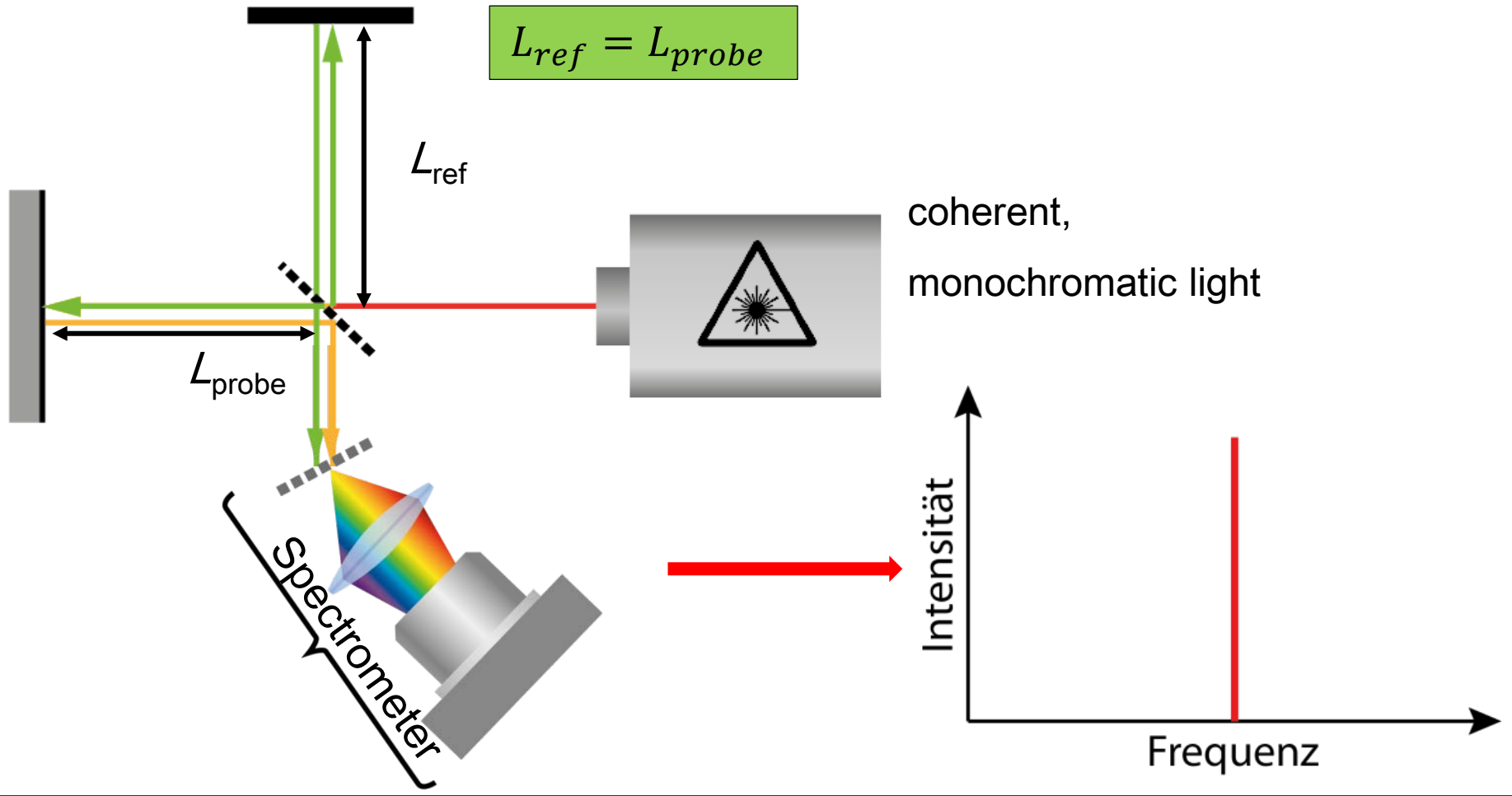
What can be measured in the time domain, can also be measured in the frequency domain.

Evolution of TD-OCT to OCT in the Frequency Domain (FD-OCT)

FD-OCT:

- Broadband, low coherence light passes an interferometer with **fixed(!)** reference arm and standard sample arm
- We then have different interference signals for the various spectral components, as they will experience different optical path lengths. (“blue with blue vs red with red”)
- One obtains with one measurement all backscattering information from all depths of the sample.
- The depth information are encoded in the modulation of the interference signal.
- By means of an (inverse) Fourier transform the backscattering information for various sample depths can be retrieved from the modulated spectrum

FD-OCT-Signal (I) : Michelson-Interferometer with Monochromatic Light

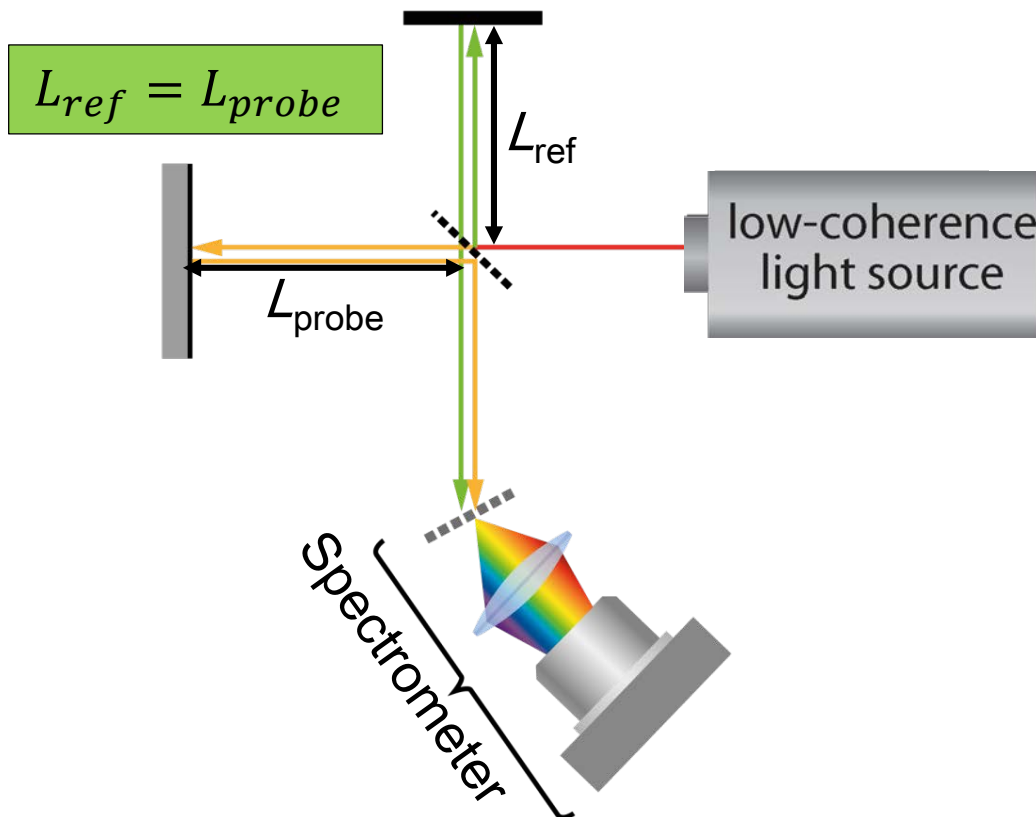


FD-OCT-Signal (II) : Michelson-Interferometer with Broadband Light

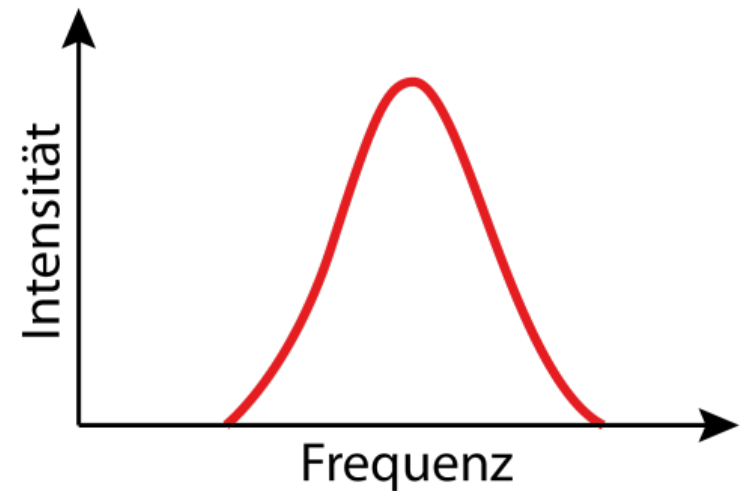
Reference- and sample path lengths are equal.

At $L_{ref} = L_{probe}$ there is constructive interference for **each single** wavelength.

At the spectrometer the superposition of all these signals is measured.



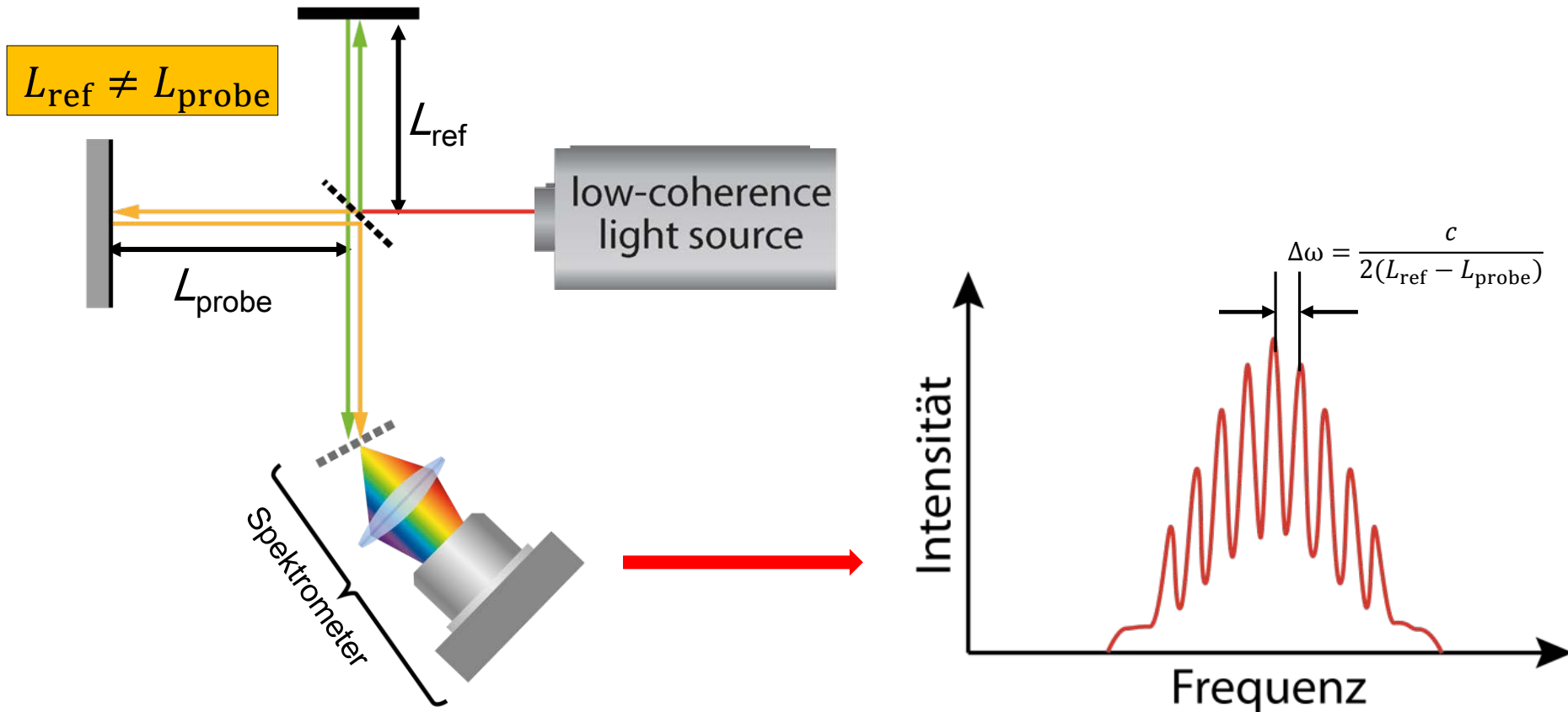
Low coherence,
polychromatic light
(spectral distribution e.g. Gaussian)



FD-OCT-Signal (III): Michelson-Interferometer „mis-matched“, Broadband Light

$L_{ref} \neq L_{probe}$ („mis matched“ interferometer):

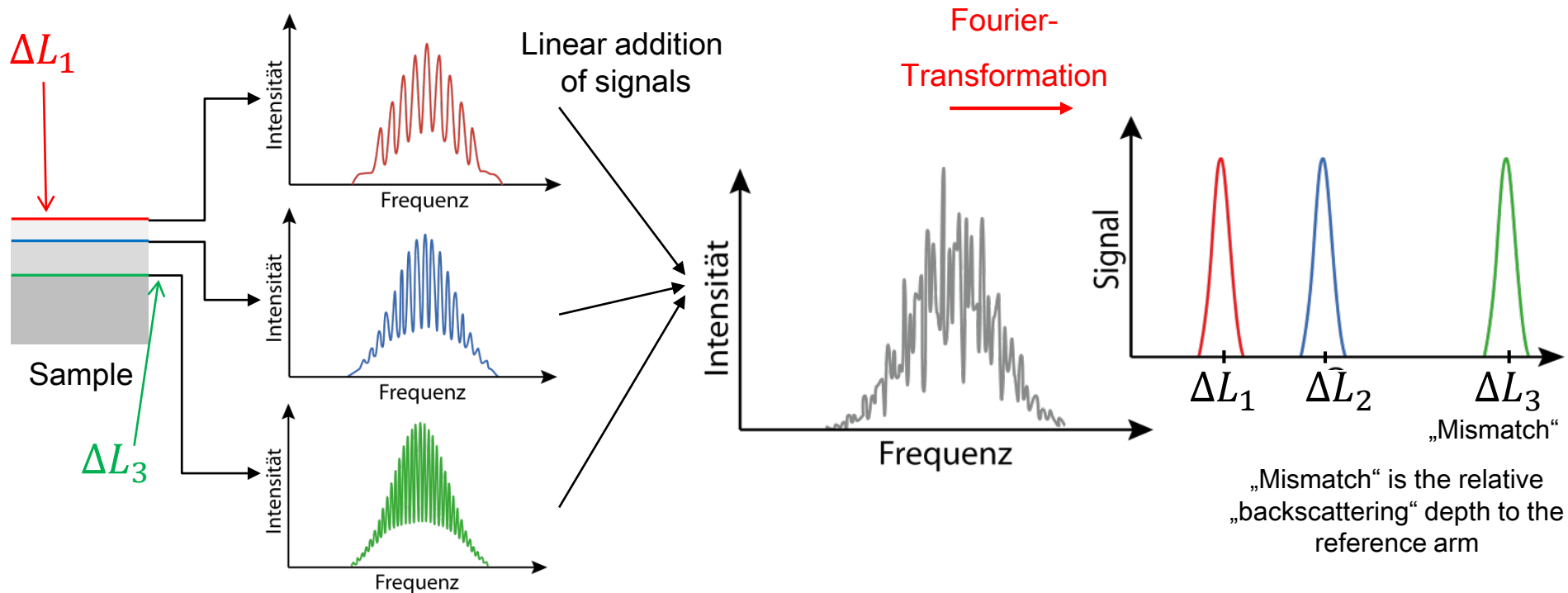
If reference and sample path show different path lengths, the individual frequency components of the broadband spectrum interfere differently. We then obtain modulations on the original Gaussian spectrum, the periods depend on the path length mismatch (i.e. sample depth).



FD-OCT-Signal (IV) : Michelson-Interferometer with various backscattering layers.

Broadband light and various layers of backscattering (real conditions):

The modulated spectra for various backscattering layers (depths) of the sample add up to a complex spectrum (linear superposition). By an inverse Fourier transform the modulations can be „translated“ into backscattering depth information of the sample.



FD-OCT: Theory I

The wave functions for both arm of the Michelson read (taking into account all backscatterers in the sample):

$$\psi_R(\omega) = \psi_{R,0}(\omega) R_R e^{2ik_R(\omega)z_R - i\omega t},$$

$$\psi_S(\omega) = \psi_{S,0}(\omega) \int_{-\infty}^{\infty} R_S(z_S) e^{2ik_S(\omega)z_S - i\omega t} dz_S$$

Disregard dispersion.

$$k = \frac{2\pi}{\lambda} = \frac{\omega}{c} = \frac{k_R}{n_R} = \frac{k_S}{n_S}.$$

Backscatterers as delta function reflection planes.

$$R_S(z_S) = \sum_i R_S(z_{Si}) \delta(z_S - z_{Si}).$$

Interference at detector:

$$I_{\text{FD}}(k) = |\psi_R(kc) + \psi_S(kc)|^2$$

FD-OCT: Theory II

$$I_{\text{FD}}(k) = \underbrace{S(k) R_R^2}_1 + \underbrace{2 S(k) R_R \int_{-\infty}^{\infty} R_S(z_S) \cos(2k(n_S z_S - z_R)) dz_S}_2 + \underbrace{S(k) \left| \int_{-\infty}^{\infty} R_S(z_S) e^{2ik(n_S z_S)} dz_S \right|^2}_3 .$$

Interference signal at detector as function of wavenumber.

1. Signal from the reference arm which is also measured if the sample arm is blocked.
2. Cross-interference signal between sample and reference arms, which is only measured if light from both arms reach the detector (spectrometer).
3. Interference between signals from backscatterers at various depths z_S . This signal is also measured even when the reference arm is blocked.

FD-OCT: Theory III

$$I_{\text{FD}}(k) = \underbrace{S(k)R_{\text{R}}^2}_1 + \underbrace{2S(k)R_{\text{R}} \int_{-\infty}^{\infty} R_{\text{S}}(z_{\text{S}}) \cos(2k(n_{\text{S}}z_{\text{S}} - z_{\text{R}})) dz_{\text{S}}}_2 + \underbrace{S(k) \left| \int_{-\infty}^{\infty} R_{\text{S}}(z_{\text{S}}) e^{2ik(n_{\text{S}}z_{\text{S}})} dz_{\text{S}} \right|^2}_3.$$

$$\hat{R}_{\text{S}}(z_{\text{S}}) = \begin{cases} R_{\text{S}}(z_{\text{S}}) & \text{if } z_{\text{S}} \geq 0, \\ R_{\text{S}}(-z_{\text{S}}) & \text{if } z_{\text{S}} \leq 0. \end{cases}$$

Use this to simplify the above equation.



$$I_{\text{FD}} = S(k)R_{\text{R}}^2 + \underbrace{S(k)R_{\text{R}} \int_{-\infty}^{+\infty} \hat{R}_{\text{S}}(z_{\text{S}}) e^{2ik(n_{\text{S}}z_{\text{S}})} dz_{\text{S}}}_{\text{cross-correlation term}} + \frac{1}{4}S(k) \left| \int_{-\infty}^{+\infty} \hat{R}_{\text{S}}(z_{\text{S}}) e^{2ik(n_{\text{S}}z_{\text{S}})} dz_{\text{S}} \right|^2.$$

FD-OCT: Theory IV

We normalize the coordinates with respect to the refractive index:

$$z_S = \frac{\hat{z}_S}{2n_S},$$

$$\hat{z}_S = 2n_S z_S,$$

$$dz_S = \frac{d\hat{z}_S}{2n_S}$$



and consider only the cross-correlation term:



$$\begin{aligned} I_{\text{FD,cc}}(k) &= S(k) R_R \int_{-\infty}^{+\infty} \hat{R}_S(z_S) e^{ikz_S 2n_S} dz_S \\ &= S(k) R_R \int_{-\infty}^{+\infty} \hat{R}_S \left(\frac{\hat{z}_S}{2n_S} \right) e^{ik\hat{z}_S} \frac{d\hat{z}_S}{2n_S} \\ &= \frac{S(k) R_R}{2n_S} \int_{-\infty}^{+\infty} \hat{R}_S \left(\frac{\hat{z}_S}{2n_S} \right) e^{ik\hat{z}_S} d\hat{z}_S \end{aligned}$$

FD-OCT: Theory V

By using the Fourier transform

$$\mathcal{F}_k\{\hat{R}_S(\hat{z}_S)\} = \int_{-\infty}^{+\infty} \hat{R}_S(\hat{z}_S) e^{ik\hat{z}_S} d\hat{z}_S$$

the cross-correlation term becomes:

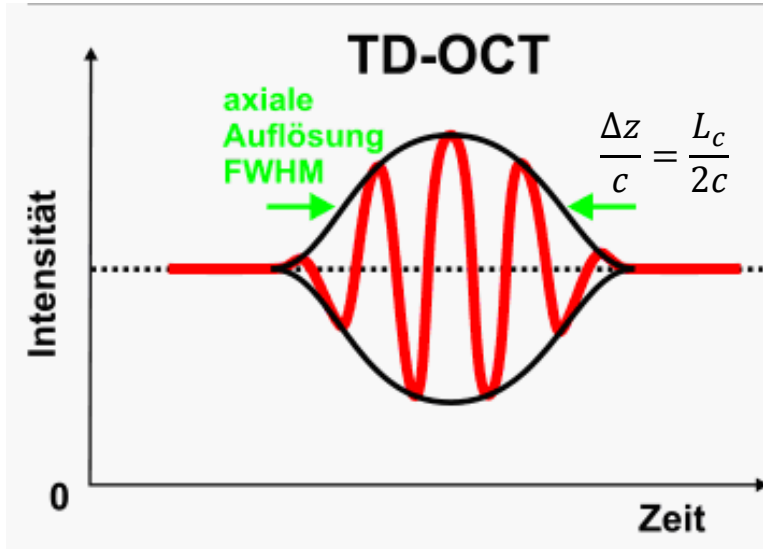
$$\begin{aligned} I_{\text{FD,cc}}(k) &= \frac{S(k)R_R}{2n_S} \cdot \mathcal{F}_k \left\{ \hat{R}_S \left(\frac{\hat{z}_S}{2n_S} \right) \right\} \\ &= \frac{R_R}{2n_S} \cdot S(k) \cdot \mathcal{F}_k \left\{ \hat{R}_S \left(\frac{\hat{z}_S}{2n_S} \right) \right\} \end{aligned}$$

FD-OCT: Theory VI

Finally the cross-correlation term becomes:

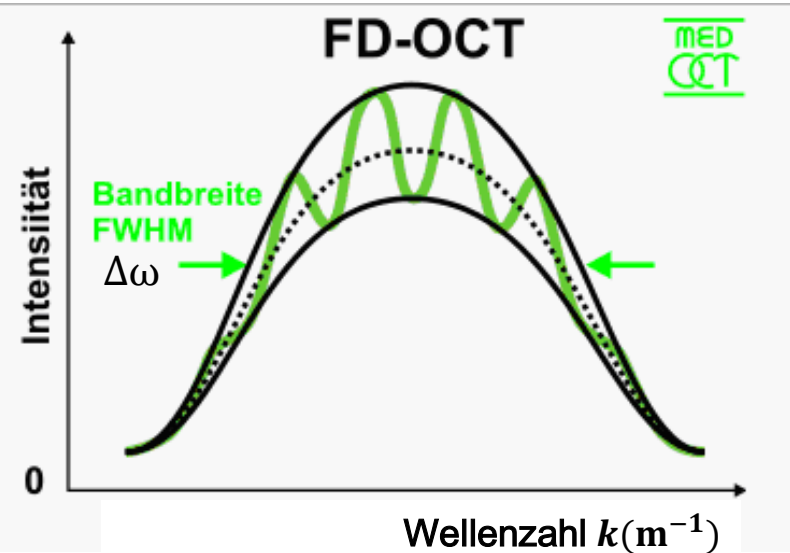
$$\begin{aligned}
 \mathcal{F}_k^{-1} \{ I_{\text{FD,cc}}(k) \} &= \frac{R_R}{2n_S} \cdot \mathcal{F}_k^{-1} \left\{ S(k) \cdot \mathcal{F}_k \left\{ \hat{R}_S \left(\frac{\hat{z}_S}{2n_S} \right) \right\} \right\} \\
 &= \frac{R_R}{2n_S} \cdot \mathcal{F}_k^{-1} \{ S(k) \} \otimes \mathcal{F}_k^{-1} \left\{ \mathcal{F}_k \left\{ \hat{R}_S \left(\frac{\hat{z}_S}{2n_S} \right) \right\} \right\} \\
 &= \frac{R_R}{2n_S} \cdot \mathcal{F}_k^{-1} \{ S(k) \} \otimes \left\{ \hat{R}_S \left(\frac{\hat{z}_S}{2n_S} \right) \right\}.
 \end{aligned}$$

Comparison Time-Domain and Frequency-Domain-OCT



Signal:
AC-signal as function of scanning time (= pathlength difference of scanned reference arm)

$$R(\Delta z) \sim I(\Delta z)$$



Signal:
Interference signal as function of wavelength or wavenumber k

$$R(z) \sim \text{FT}[I(k)]$$

To be obtained

Advantage Frequency-Domain-OCT: High Definition and High Resolution

- **Simple mechanics:** All backscattering signals along z-axis (A-Scan) are available simultaneously, no moving parts.
- **Sensitivity:** Parallel measurement with diffraction grating and CCD. The Fourier-transformed signals of each CCD-pixel add up coherently, whereas the noise components add up incoherently → higher Signal-to-Noise Ratio (SNR) by factor N (number of spectrometer channels)*
- **Speed:** Because each Fourier transformation yields the complete A-scan, FD-OCT allows the scan of larger 3D-volumes compared to TD-OCT → less artefacts of obtained image due to sample movements (eye

* $N/2$, as Fourier transformation contains positive and negative frequencies, both carrying the same information

Time Domain

Frequency Domain

Used terminology	Scanning TD-OCT	Spectral-domain OCT, Fourier-domain OCT	swept-source OCT
z scan	sequential in time	parallel	sequential in time
Type of z scan	moving reference mirror, rapid scanning optical delay line (RSOD)	no moving part	no moving part
Light source	superluminescent diode, low-coherence laser	superluminescent diode, low-coherence laser	tunable wavelength light source
Detector	diode, avalanche photodiode	prism or grating and line detector	diode, avalanche photodiode
Interferometer	beam splitter	beam splitter	beam splitter
A-scans/s	4000	25 000–300 000	100 000–1 000 000
Voxels/s	10 000–100 000	20–40 million	100–2500 million

Spectral Domain and SS-OCT have dramatic signal-to-noise advantages

Time Domain OCT

Spectral Domain OCT

Detection in N wavelength channels

Fourier Domain OCT

Swept Source OCT

Shot-
noise-
limited
detection

$$\text{SNR}_{\text{TD-OCT}} = \frac{\langle I_{\text{TD}} \rangle^2}{\sigma_{\text{sh}}^2} = \frac{T \eta \mathcal{R}_S}{h \nu_0 B} P_0$$

$$\text{SNR}_{\text{FD-OCT}} = \frac{\langle i_{\text{D}} \rangle^2}{\sigma^2[z_{\text{n}}]} = \frac{\eta}{h \nu_0} \frac{\mathcal{R}_S}{B_{\text{FD}}} P[k_{\text{n}}] N$$

...

... can be
achieved

$$\text{SNR}_{\text{SS-OCT}} = \text{SNR}_{\text{FD-OCT}} = \frac{\eta}{h \nu_0} \frac{\mathcal{R}_S}{B_{\text{TD}}} P_0 N$$

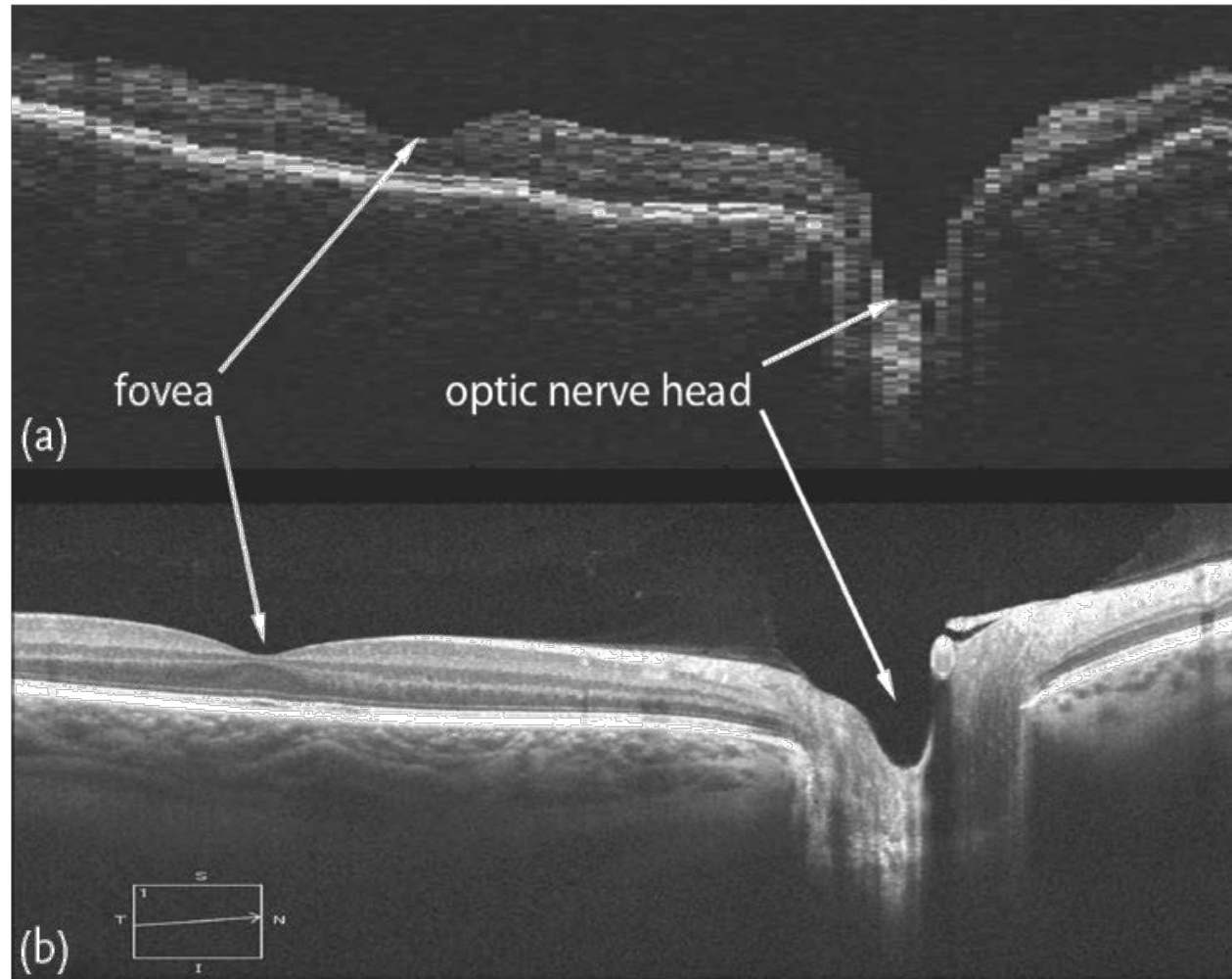
Advantage Frequency-Domain-OCT: High Definition and High Resolution



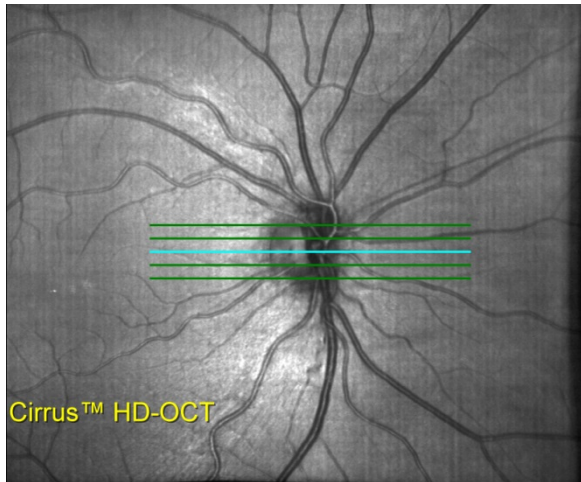
ZEISS Stratus OCT (TD-OCT)



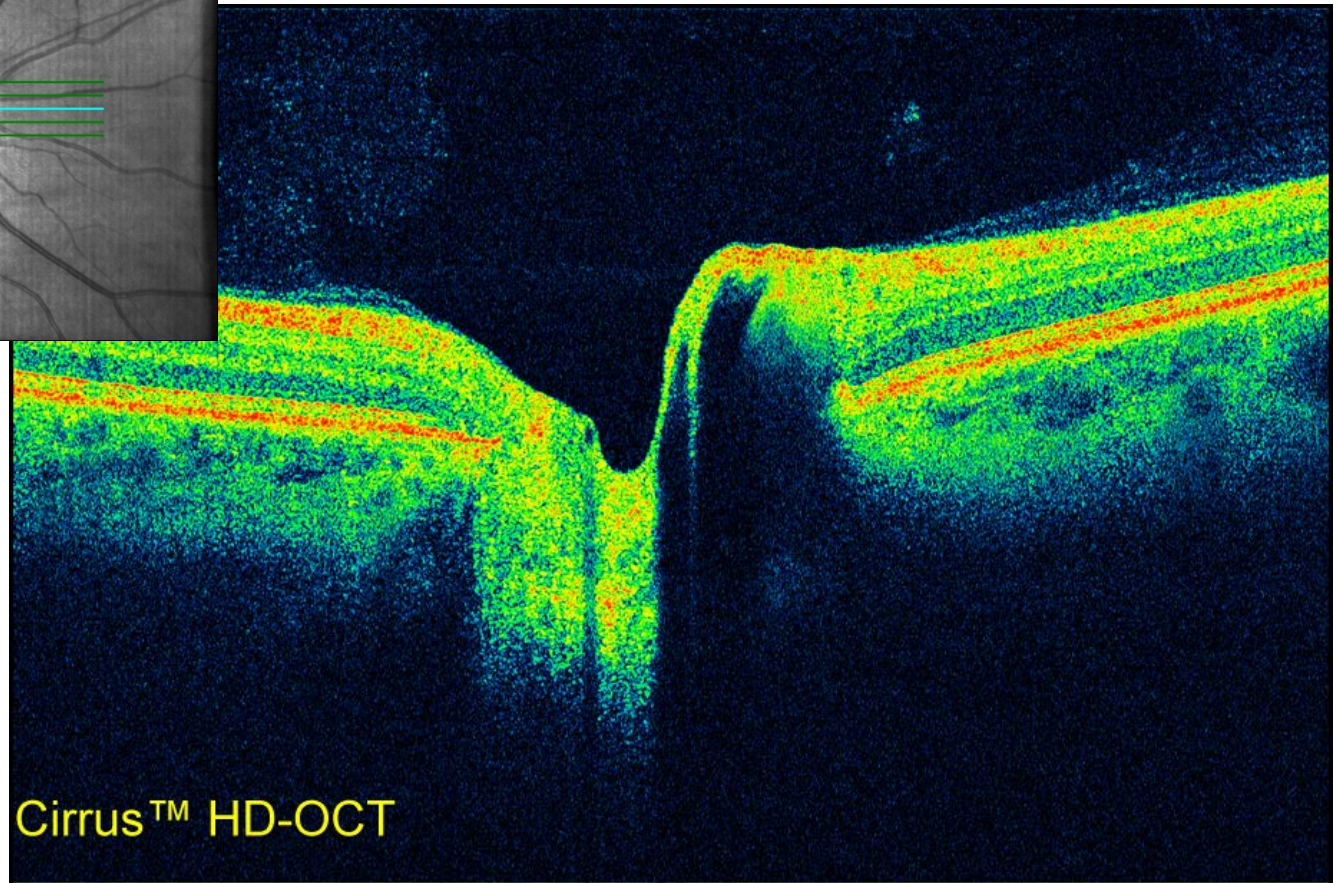
ZEISS Cirrus OCT (FD-OCT)



Advantage Frequency-Domain-OCT: High Definition and High Resolution

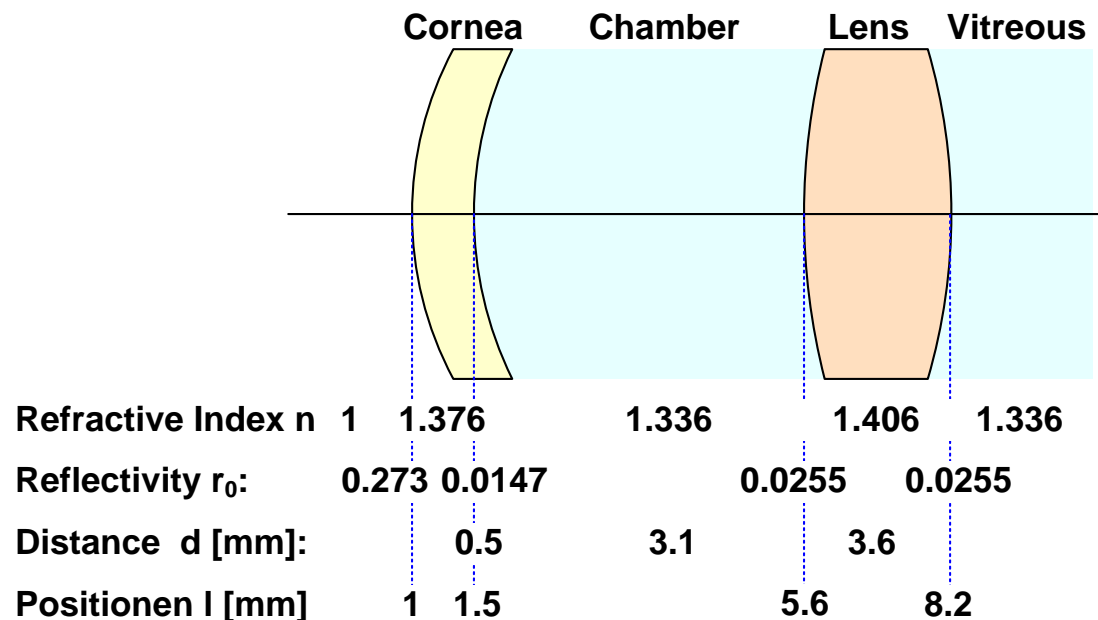


Beispiel: OCT-Scan des Sehnervenkopfs mit hoher Kontrastschärfe und hoher Auflösung

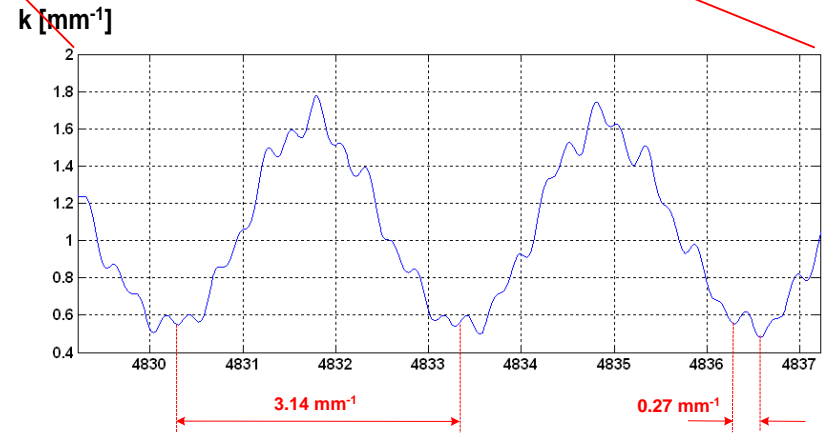
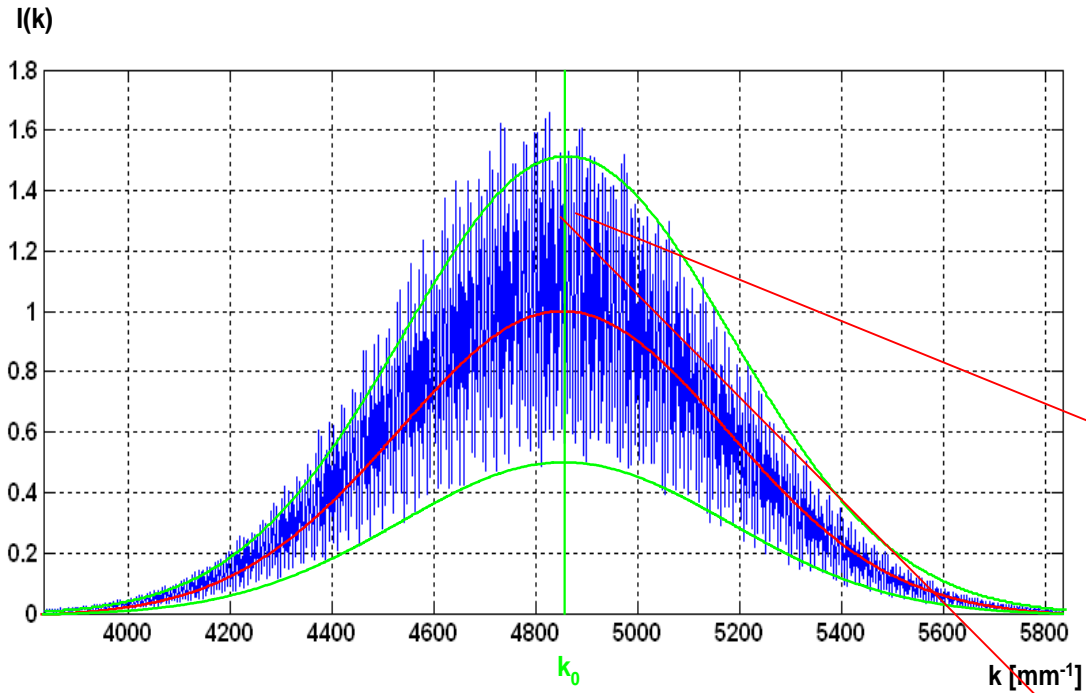


Exercise Theory of FD-OCT

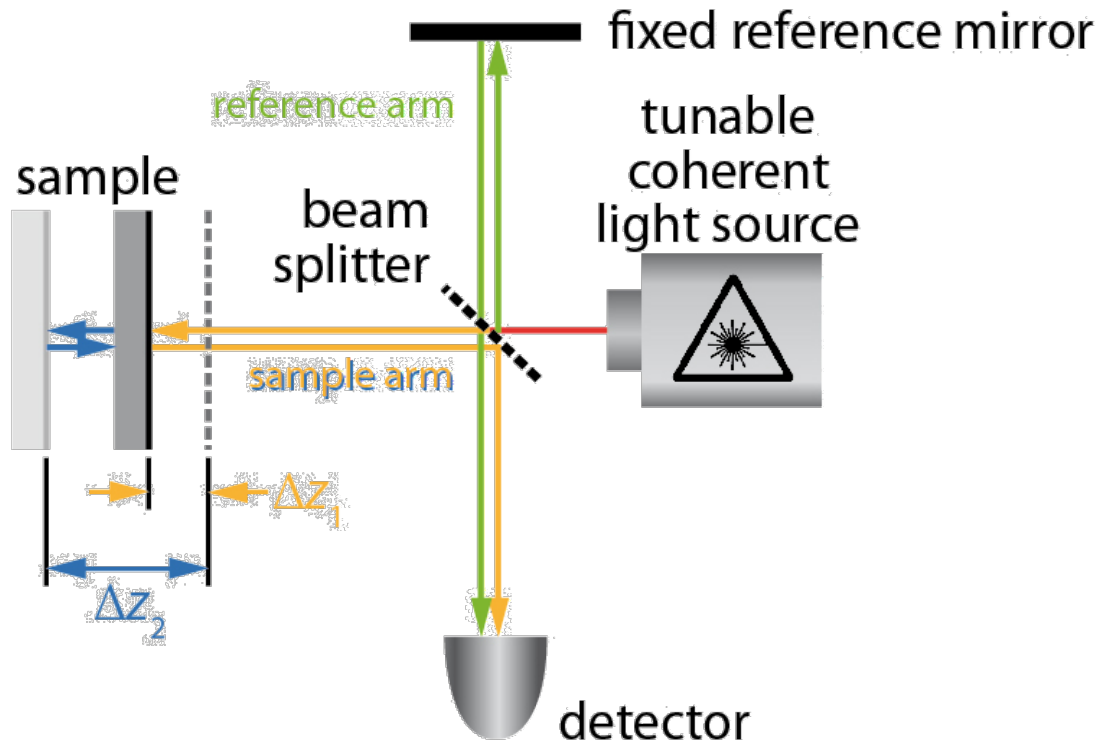
1. Use a mathematical software tool (e.g., Matlab or MathCad) to simulate an FD-OCT spectrum resulting from the reflections of the 4 major interfaces of the anterior segment of the eye (assumed to be δ functions in space). Assume a Gaussian pulse of spectral bandwidth for various broadband light sources, for example, an SLD with $\lambda_0 = 1300$ nm and 200 nm bandwidth, and an SLD with $\lambda_0 = 1050$ nm and 100 nm bandwidth and a titanium:sapphire laser with $\lambda_0 = 800$ nm and 70 nm bandwidth. What can you say about the required resolution of the spectrometer and the dynamic range?



Simulation Frequency-Domain-OCT



Evolution of FD-OCT to Swept-Source-OCT-Technologie (SS-OCT)

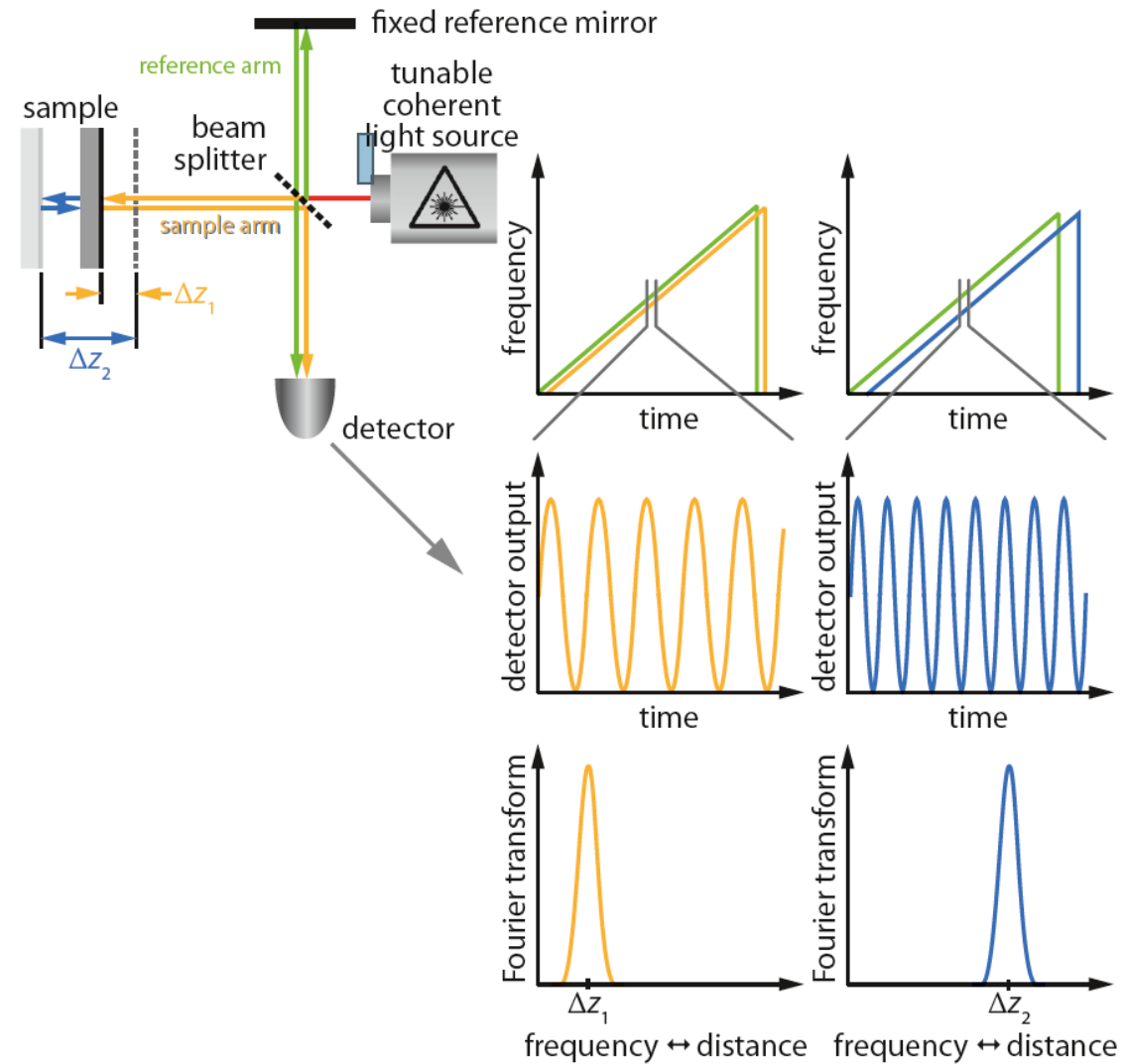
**SS-OCT:**

- Light passes through a Michelson interferometer with fixed (!) reference arm.
- The wavelength will be rapidly tuned.
- During the tuning the detector collects sequentially backscattering information of all sample depths
- The depth information is contained in each interference signal of the individual sequentially tuned spectral “colors” of the light.
- By Fourier transformation of the measured signal the backscattering structure along the z-dimension can be reconstructed (similar as in FD).

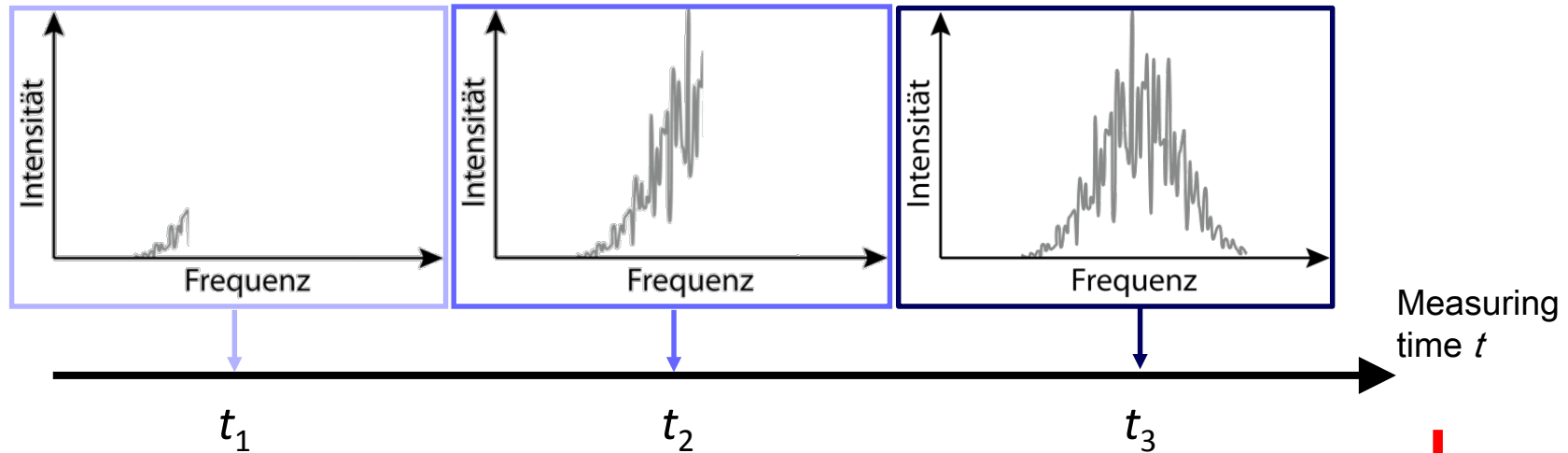
Evolution of FD-OCT to Swept-Source-OCT-Technologie (SS-OCT)

Idea:

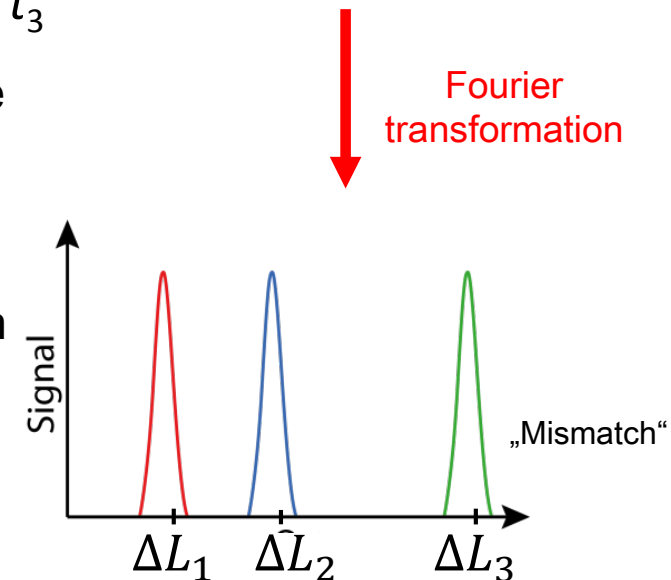
Instead of a broadband light source one uses a tunable source and instead of the spectrometer a simple diode as a sensor which measures the signal as a function of the tuned frequency over time. Time encoding is here actually frequency encoding.



SS-OCT-Signal



The signals contributing to the interference signal at time t have due to the continuous tuning (Sweep) of the source different paths and travel times to the detector and therefore different frequencies (colors). The superposition at the detector results in a beat/modulation signal which depends on the path length difference. During the Sweep the signal is sequentially build up. After completion of one Sweep the measured signal corresponds to the spectrum $I(\omega)$ of FD-OCT.



Exercise Theory of SS-OCT

Let us consider an SS-OCT with 1050 nm center wavelength and a sawtooth-like sweep.

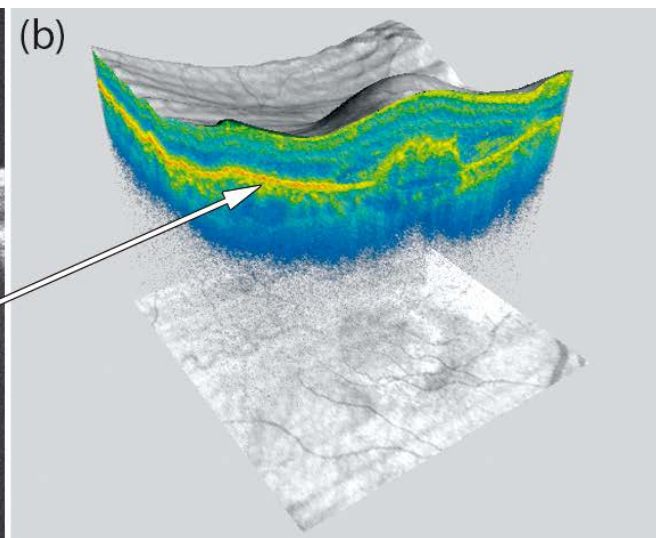
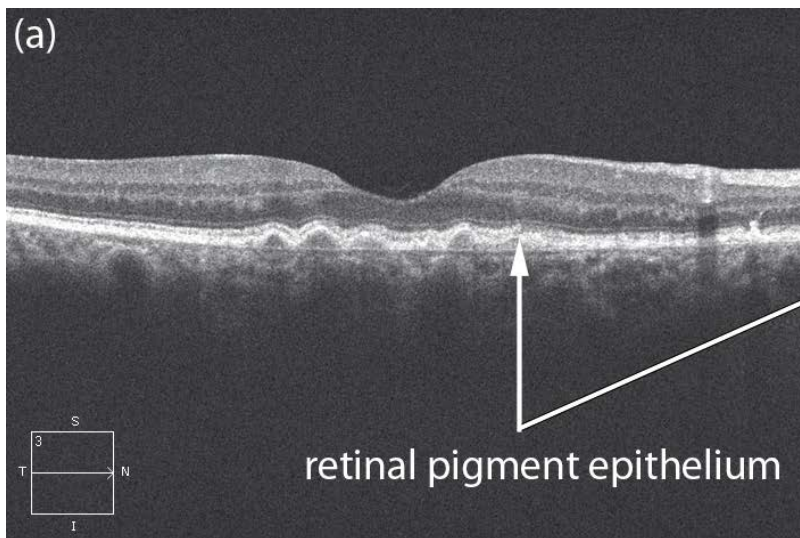
1. Use a mathematical software tool (e.g., Matlab or MathCad) to simulate the detector signal for a typical sweep rate of 200 kHz and various arm length mismatches (100 μm , 1 mm, 10 mm).
2. How does the result change when the direction of the sweep is reversed? How, if the sweep rate is reduced to 50 kHz?
3. Use a mathematical software tool (e.g., Matlab or MathCad) to simulate the SS-OCT spectrum resulting from the reflections of the 4 major interfaces of the anterior eye segment (assumed to be δ functions in space). Use 1050 nm as a center wavelength and a sawtooth-like sweep with 200 kHz. Then, Fourier transform the simulated results to obtain an A-scan of the anterior segment of the eye.

Advantages of SS-OCT

1. **Compared to TD-OCT:**
analog to FD-OCT

2. **Compared to FD-OCT:**
 - No CCD/CMOS-Kamera necessary (→ cost effective)
 - No spectrometer necessary, which limits the scan depth (and therefore z-axis depth)
 - Maximum scan depth of SS-OCT depends on bandwidth of converter and inverse Sweep-rate of the light source
 - Faster scans, as Sweep-rate of the light source is faster than read-out rate of CCD cameras

Optical Systems in Medical Technology



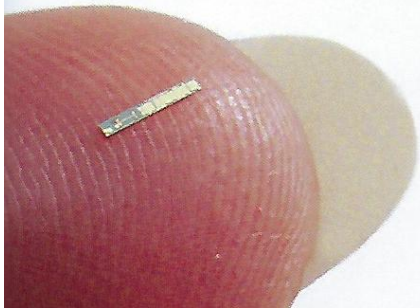
Modern Developments of Optical Coherence Tomography (OCT)

Akinetic OCT

Insight's Akinetic Swept Laser™

Revolutionizing Optical Coherence Tomography

FDML (incl. Parallelization)



* a·kin·et·ic: absence of movement



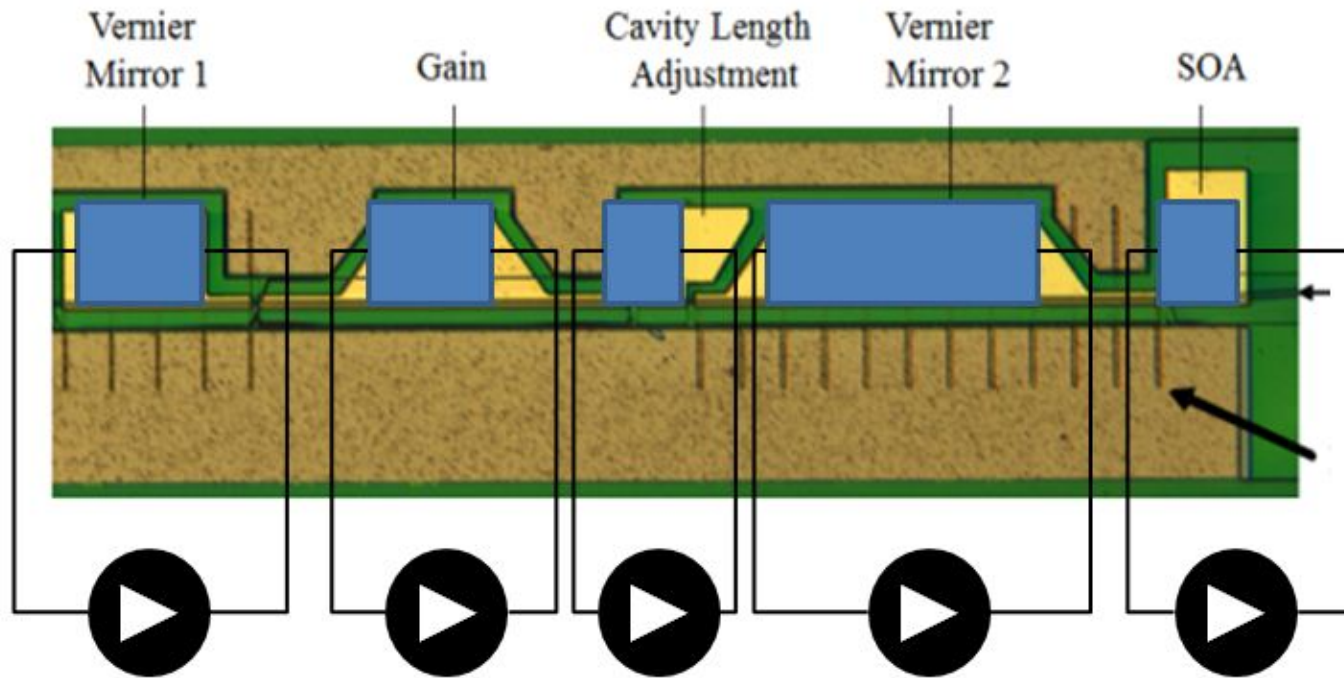
All-Semiconductor Akinetic Swept Laser™

- 2k to 400k sweeps per second
- > 220 mm coherence length, adjustable (> 110 mm imaging depth range)
- Deep point spread function and high sensitivity
- Very phase stable for better images, Doppler, angiography: ~0.5 pm RMS
- Clean images without artifacts
- Inexpensive



SweptLaser.com

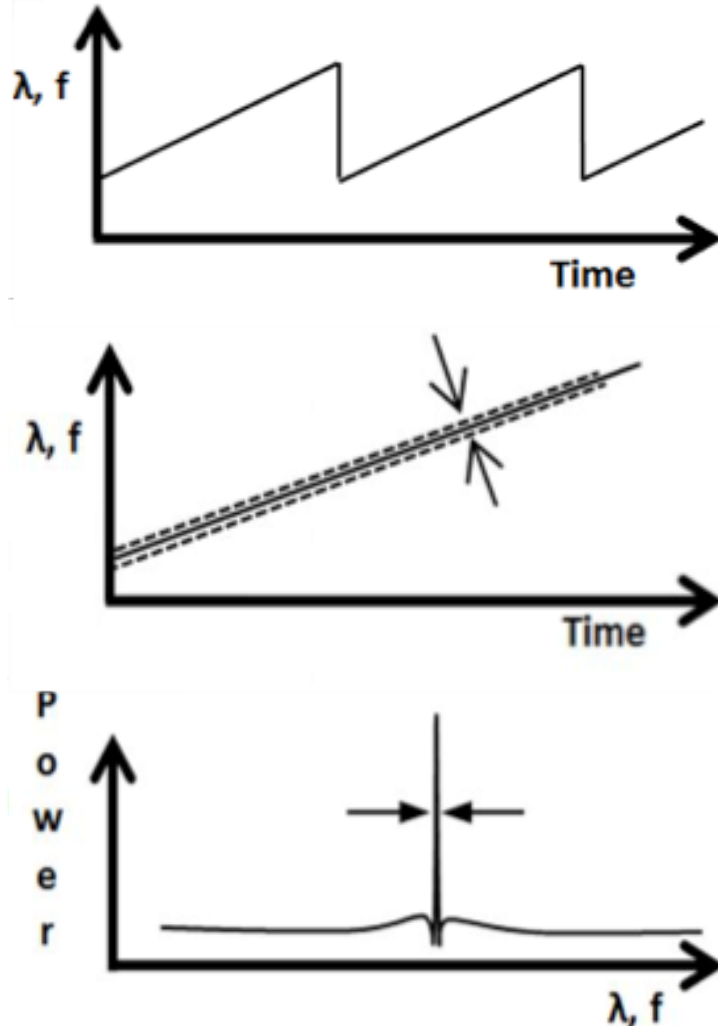
Akinetic OCT



The basic structure is an all semiconductor VT-DBR (Vernier-tuned distributed Bragg reflector) laser.

Here are five tuning elements in the laser. Tuning occurs when current is applied to a segment of the laser. This current increases the carrier density in a specific region of the device and changes the index of refraction of the material. This change in the index changes the effective length of that specific segment of the laser. Two of the segments of the laser are mirror sections (front mirror and back mirror). By applying current and changing the index of the material, the mirror spacing is (effectively) changed. Employing Vernier-tuning effect, these two mirrors can be used in combination to select any wavelength across the tuning band.

Akinetic OCT



High-Speed Sweeping

- 400k, 200k, 100k, 50k, 20k, 10k, 4k sweeps per second; adjustable to any speed 2k to 400k
- Technology demonstrated to 1M sweeps per second
- 95% duty cycle, adjustable; nanoseconds between sweeps

Sweep Linearity

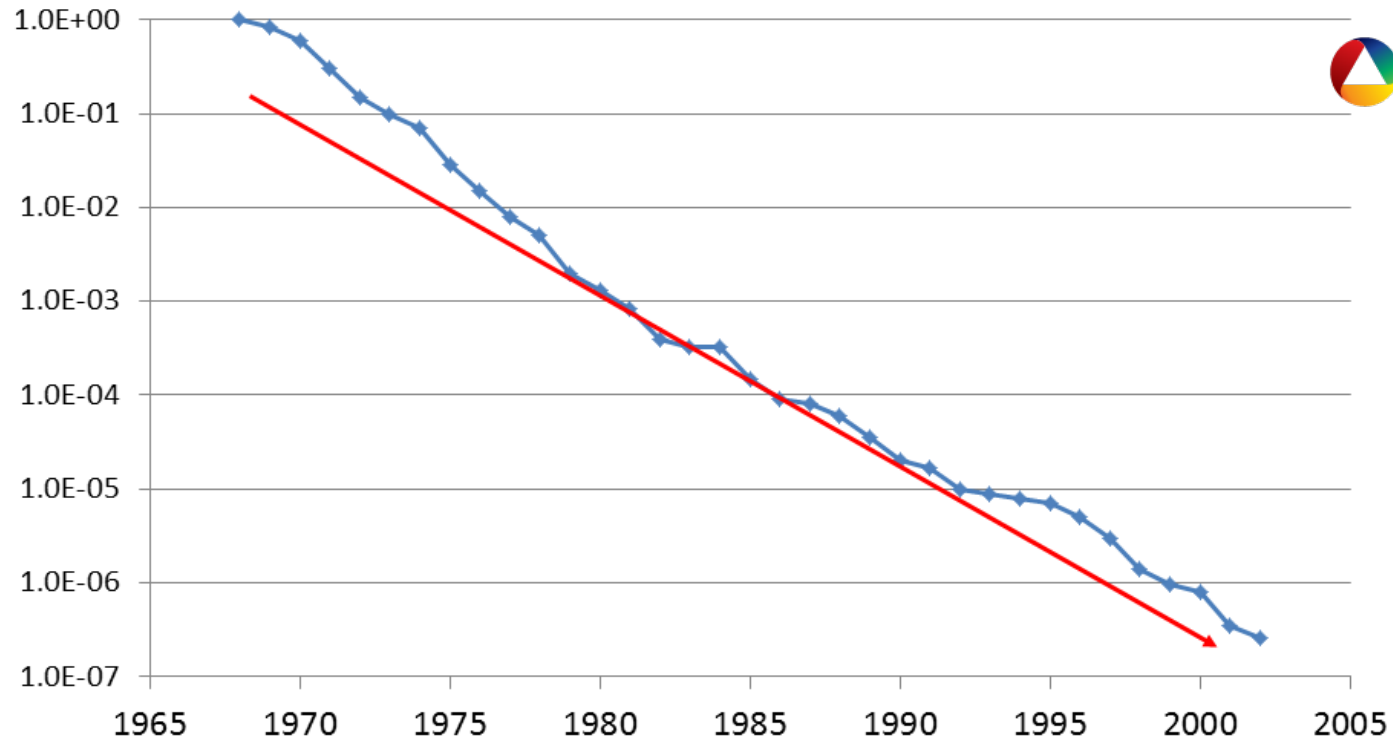
- No need for an external k-clock
- Linearity better than 0.01% at 200,000 sweeps per second (± 0.5 pm RMS; ± 0.1 GHz)
- Trigger jitter <300 femtoseconds. No mode hops.

Clean Optical Performance

- Single longitudinal mode
- Dynamic coherence length >220 mm (110 mm imaging depth range), Coherence length not dependent on sweep rate
- Clean point spread function with 55–65 dB noise floor

Akinetic OCT

Semiconductor Exponentially Declining Prices, 40 years (price per transistor)



Akinetic OCT

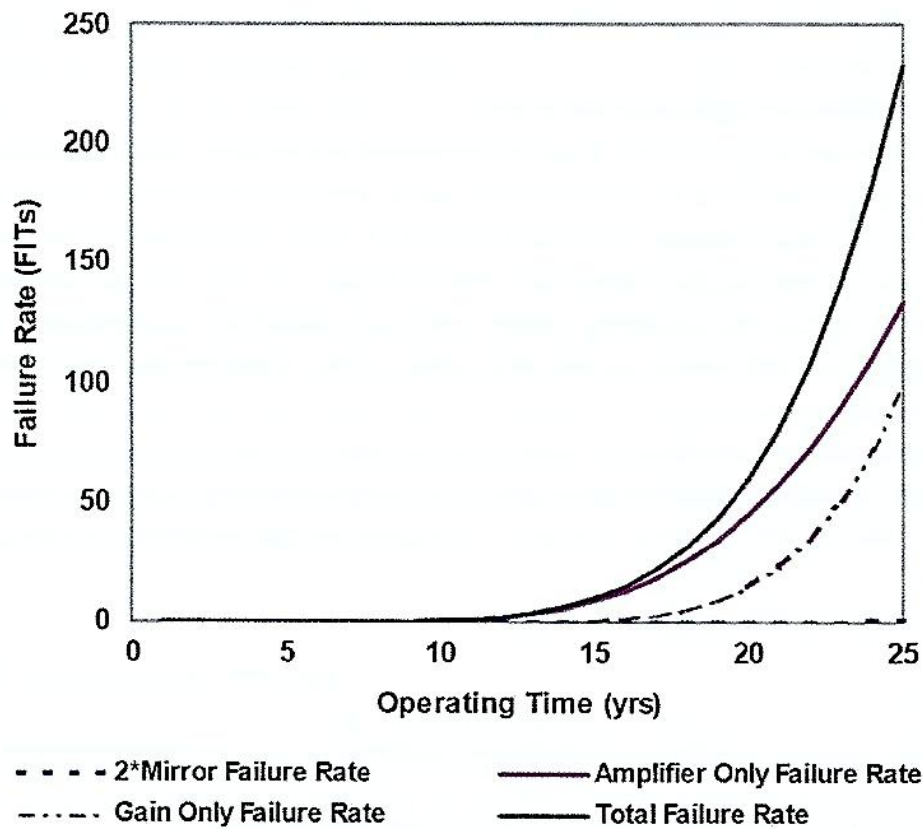
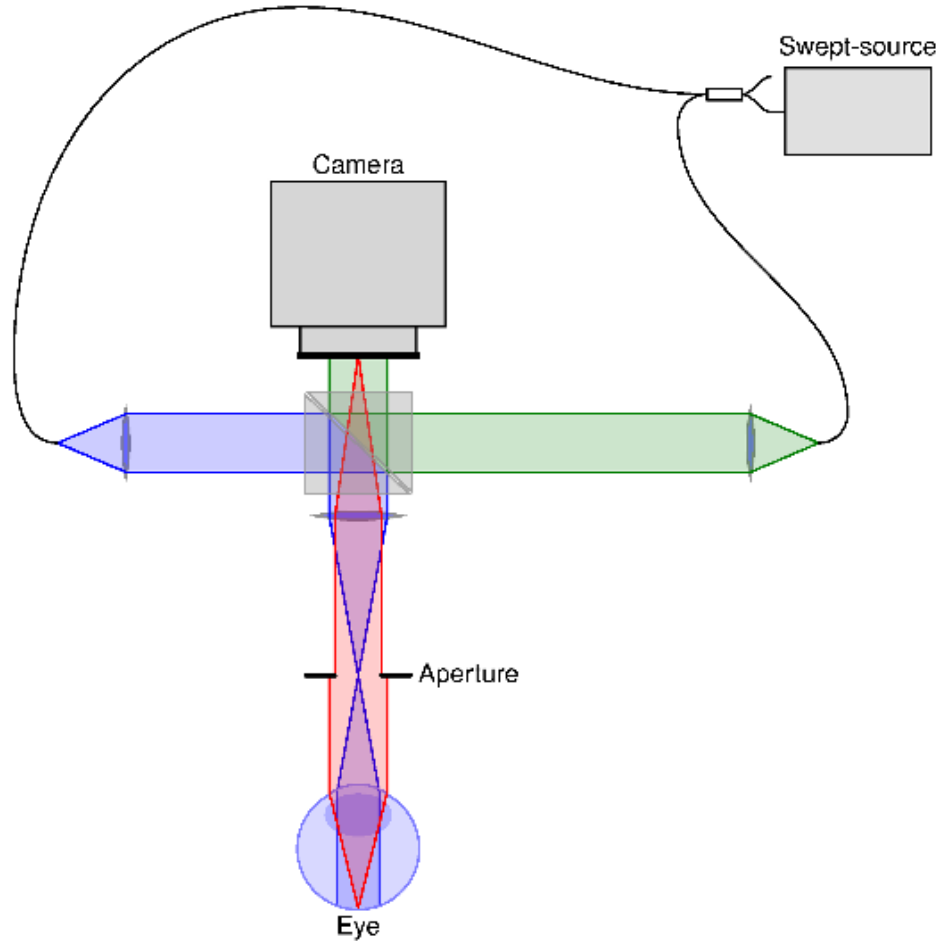


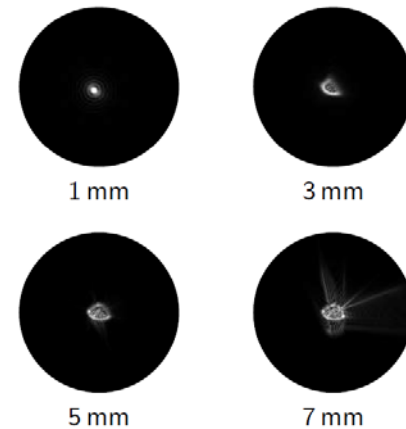
Fig. 23.38 FITs (failures per billion) of the semiconductor are minimal over 10 years and even at 15 years represent less than 20 failures per billion. The laser will likely succumb to a mechanical failure (e.g., connectors) before the laser reaches end of life. The lack of mechanical movement is a major reason for the long mean time to failure (*MTTF*)

An extended detector enables SS-OCT to simultaneously access the full field information



For instance it can be used to correct eye aberrations that prevent imaging at high lateral resolution

PSF and pupil diameter



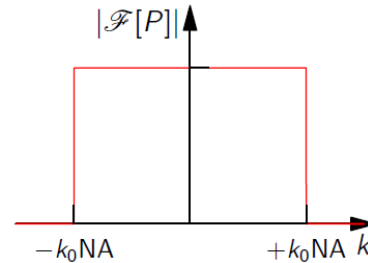
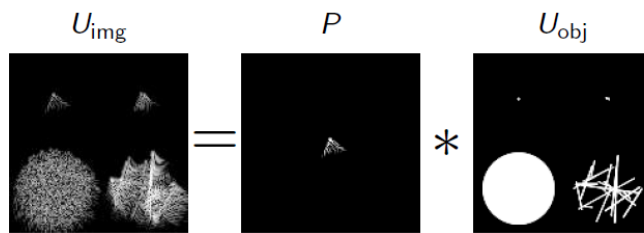
Aberration-corrected high-speed full-field swept-source OCT

D. Hillmann and G. Hüttmann et al.

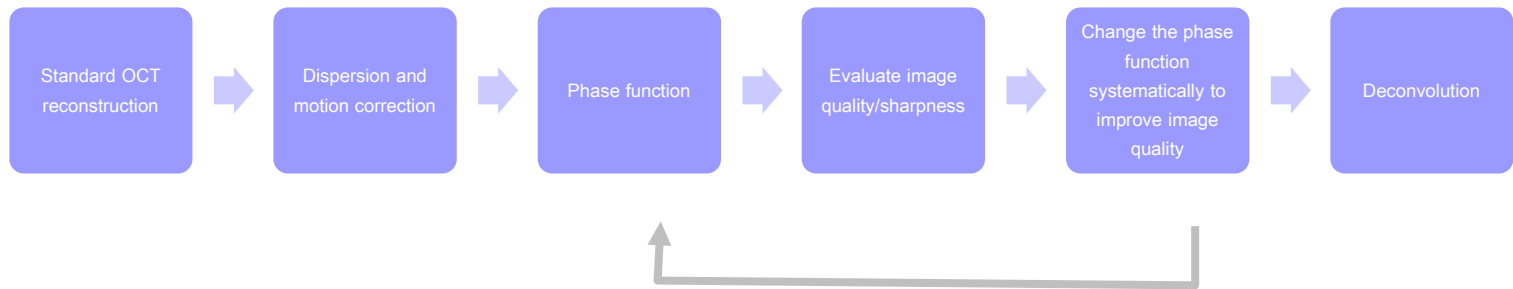
Presented at SPIE BIOS 2016

Iterative wavefront phase estimation and numerical reconstruction ...

Coherent imaging



- Amplitude Transfer Function (ATF)
- $\mathcal{F}[P] = \exp(i\phi)$
- Invertible by complex conjugation



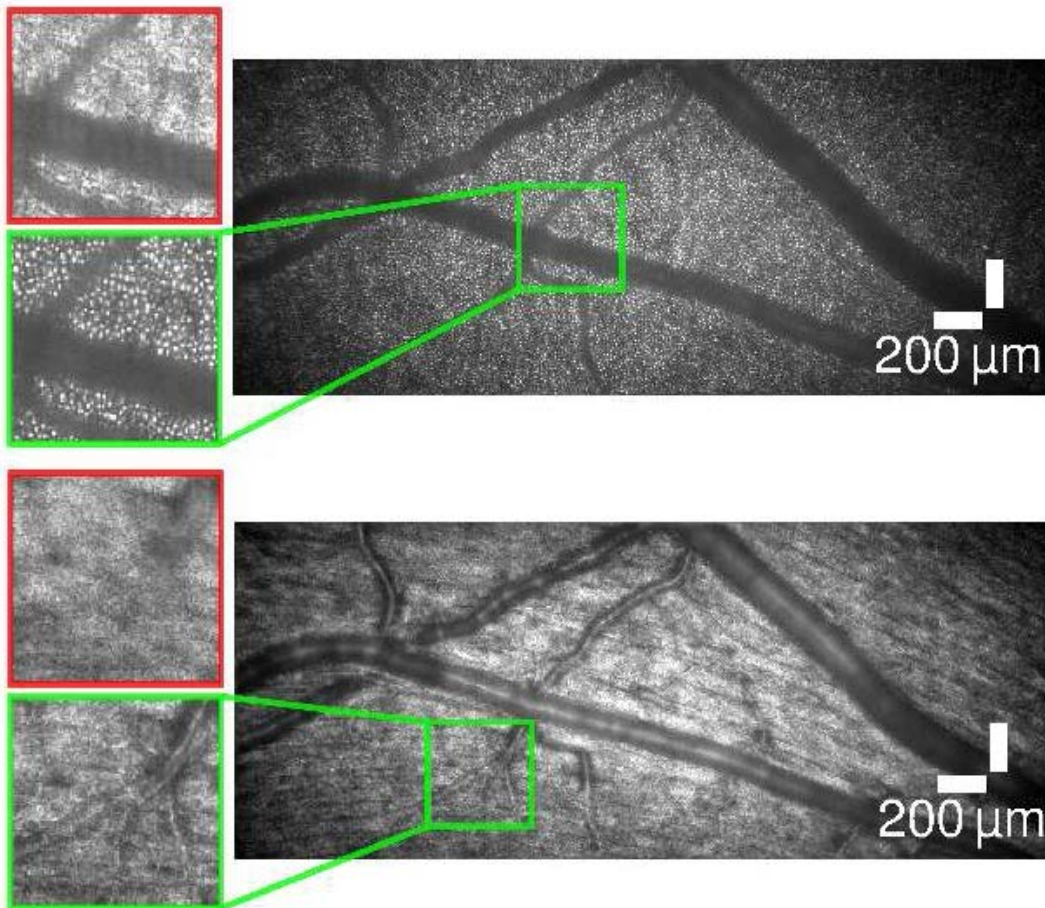
Aberration-corrected high-speed full-field swept-source OCT

D. Hillmann and G. Hüttmann et al.

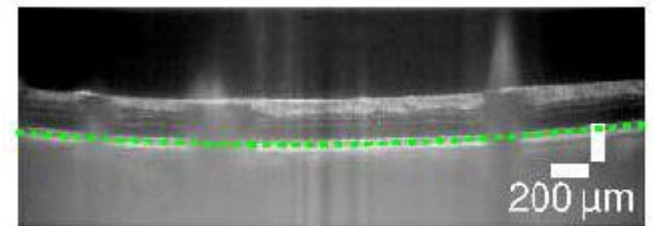
Presented at SPIE BIOS 2016

... enables diffraction limited imaging

- Imaging with 3.5 mm pupil, at 14° in periphery (healthy subject)
- Phase represented in Zernike polynomials up to 6th order

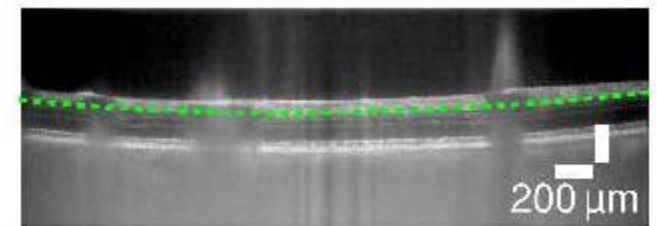


50x average and z-projection



Photoreceptors

Nerve fibers

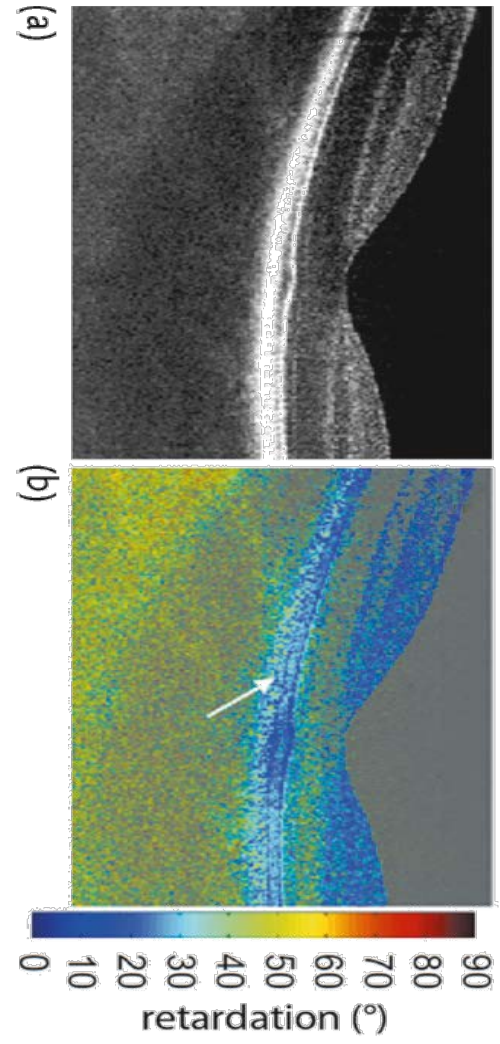
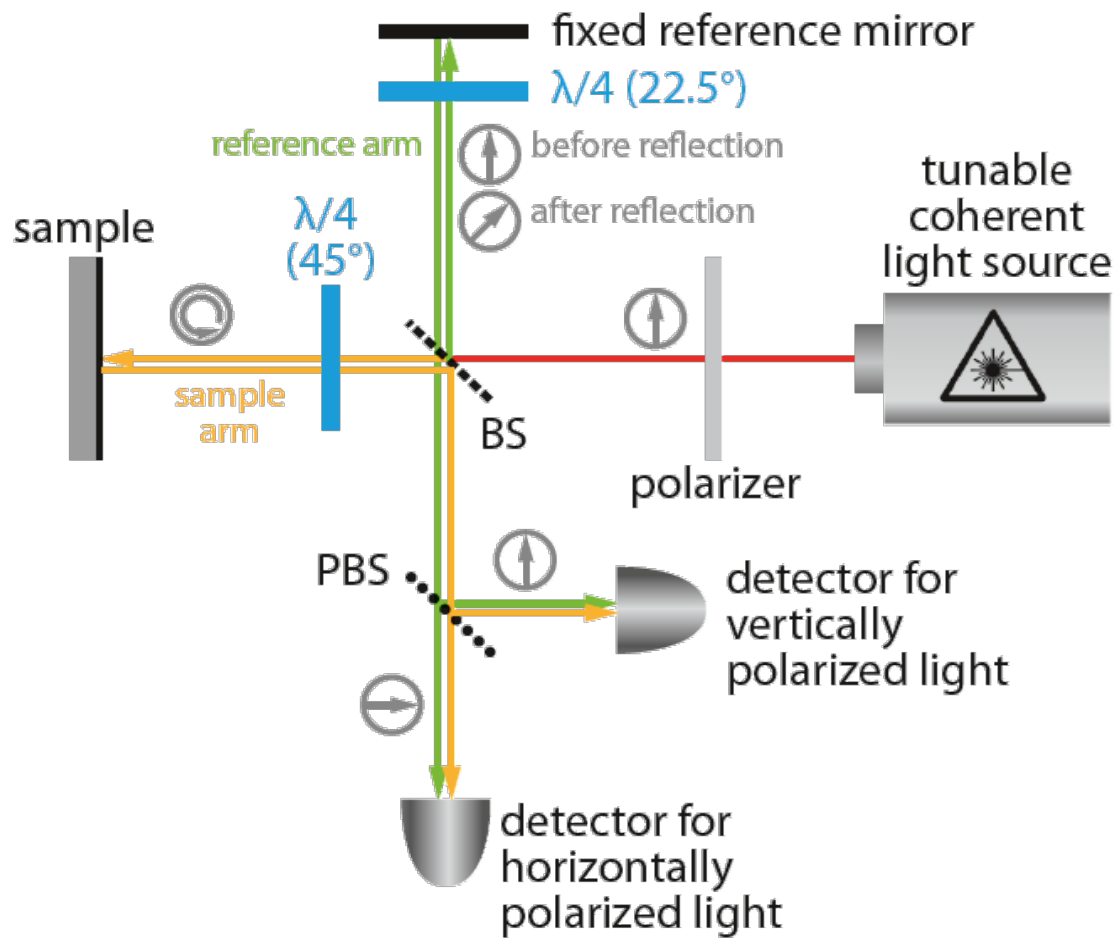


Aberration-corrected high-speed full-field swept-source OCT

D. Hillmann and G. Hüttmann et al.

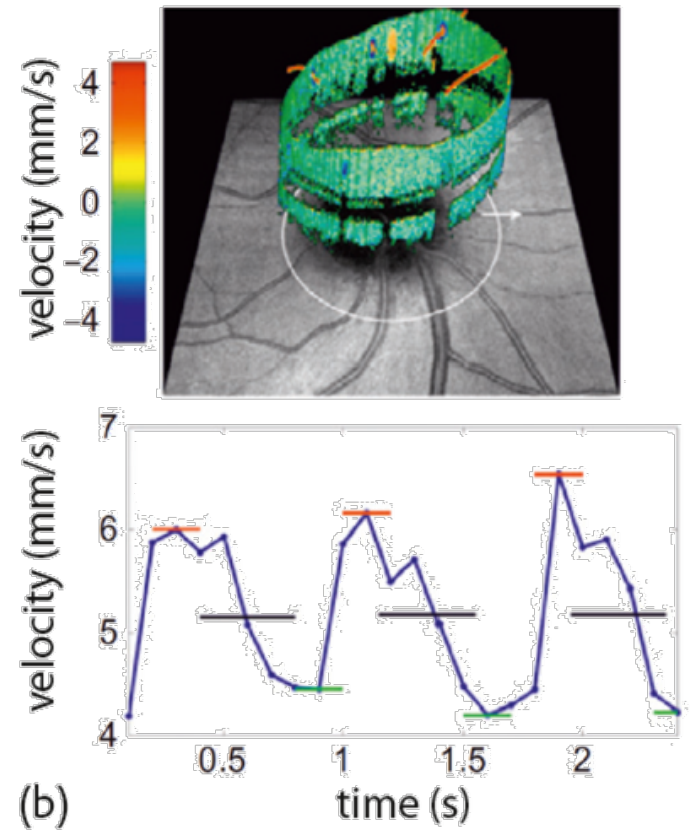
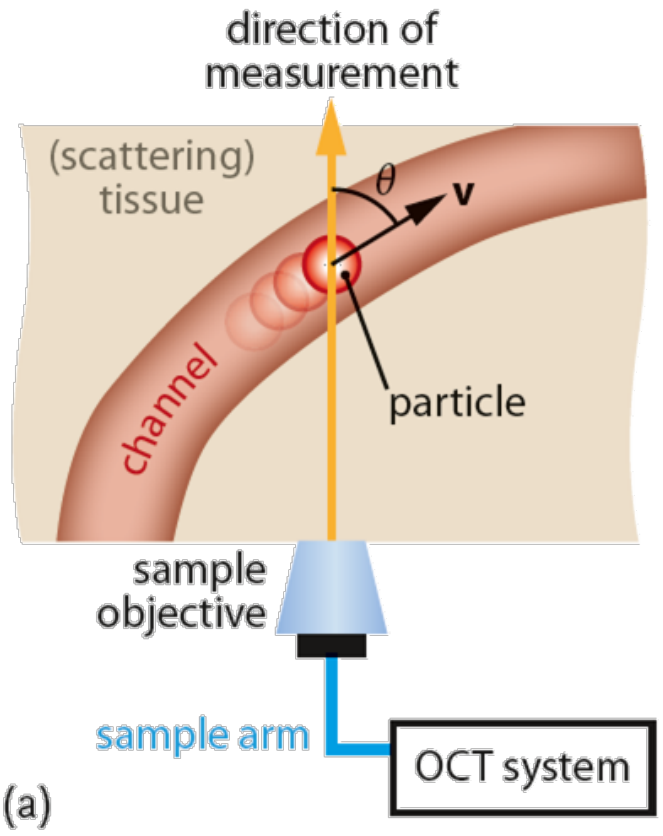
Presented at SPIE BIOS 2016

Polarization Sensitive OCT

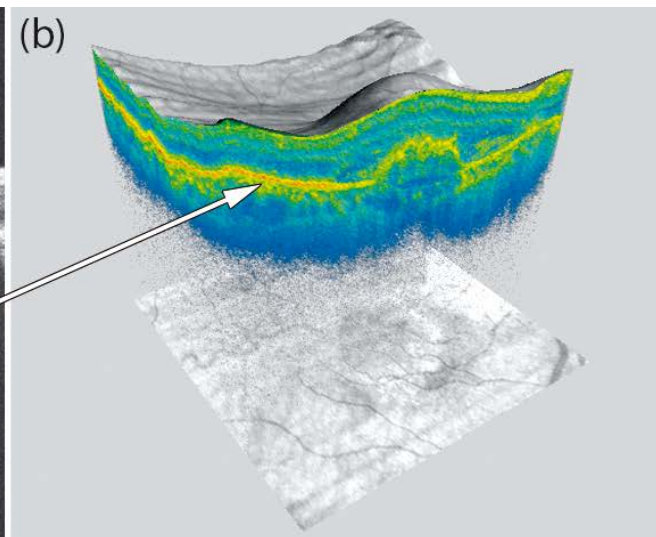
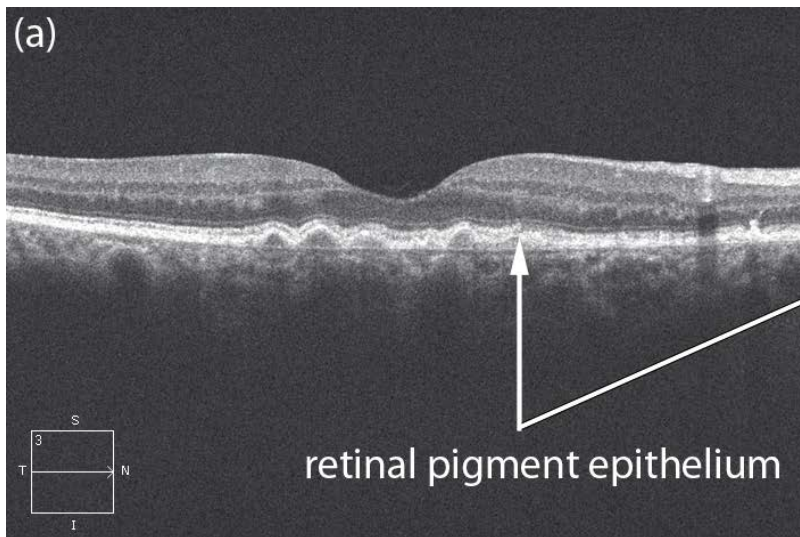


Doppler-OCT

$$v = \frac{\lambda_0 \Delta \nu_{\text{Doppler}}}{2 \cos \theta},$$



Optical Systems in Medical Technology

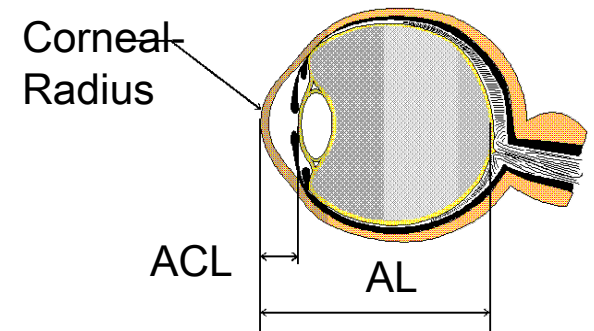


Applications of Optical Coherence Tomography (OCT)

Application 1: OCT - Biometry

Biometry:

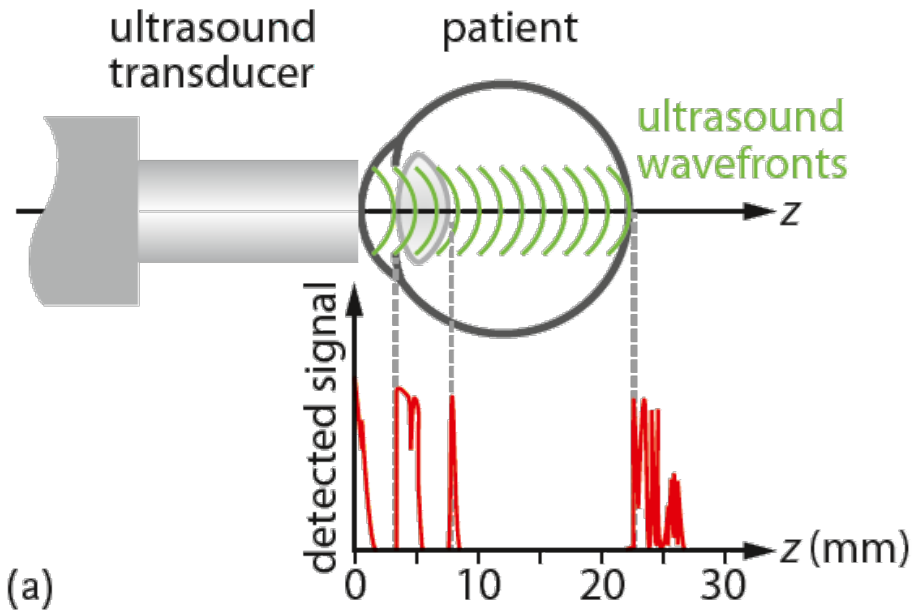
Prior to each cataract surgery both eyes need to be measured to determine the correct IOL for implantation.



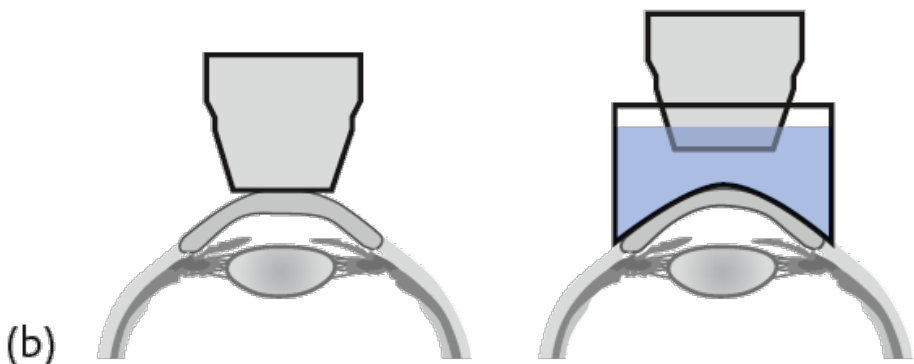
Measurable quantities are:

- **Axial length of the eye (AL)** = Eye length along the visual axis
- **Anterior Chamber Length (ACL)** = Distance Cornea-Lens
- **Radius of Curvature of cornea (Corneal-Radius)**

Application 1: OCT – Biometry: Prior Art: Ultrasound-Biometry

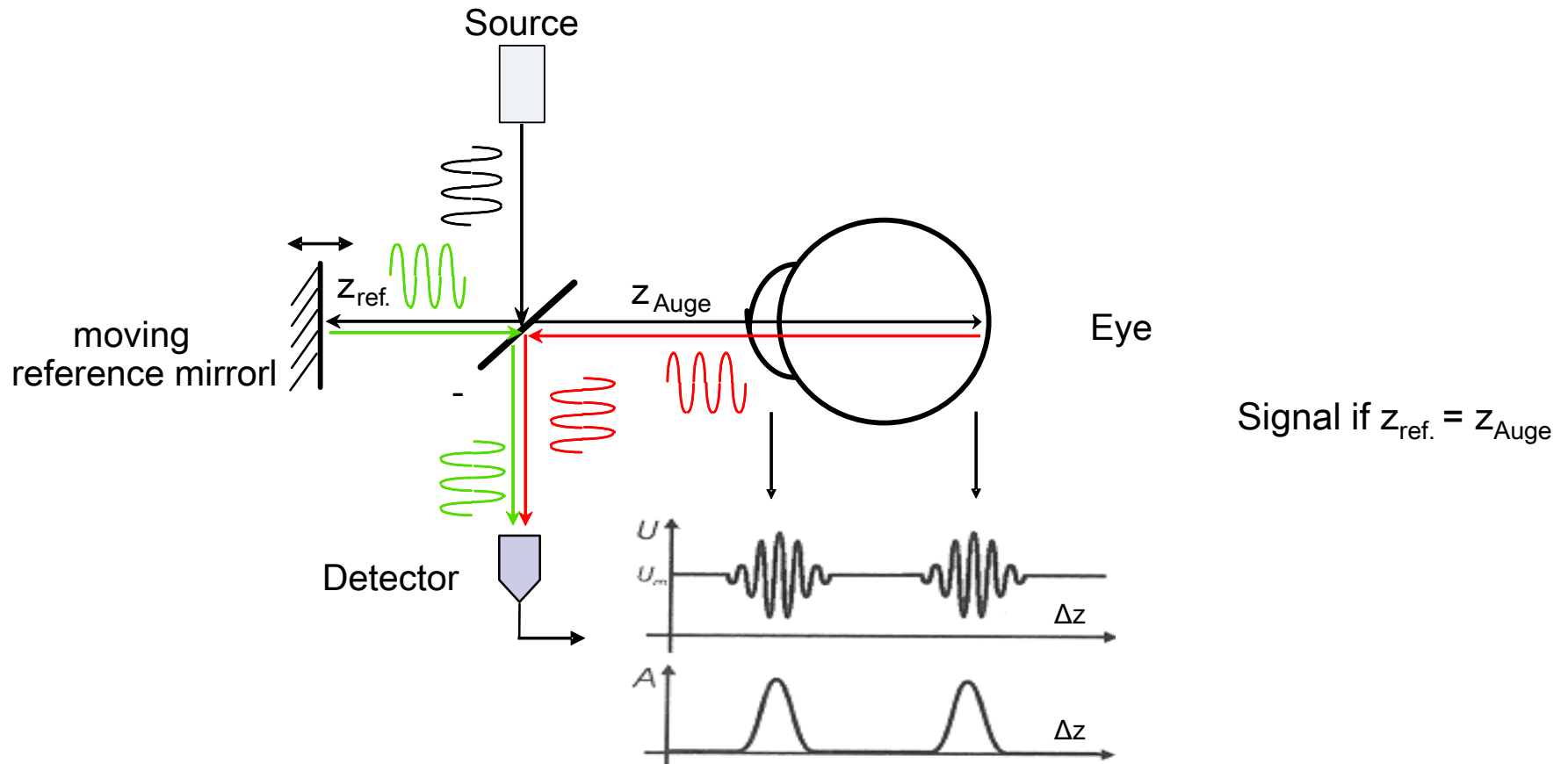


(a)



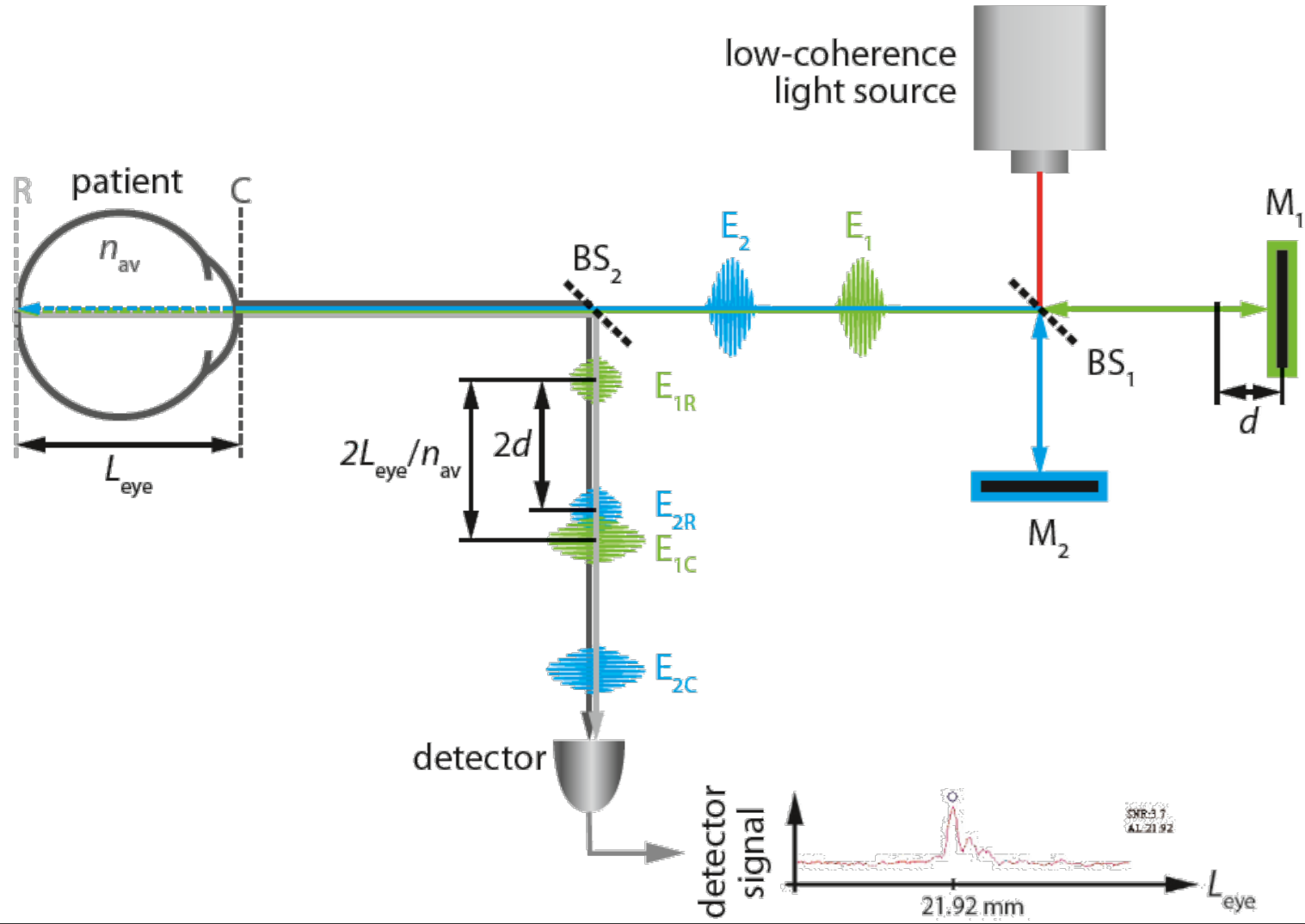
(b)

Application 1: OCT – Biometry / Eye Length Measurement



- ⇒ precise and non-invasive eye length measurement
- ⇒ **but axial relative movement of eye-instrument is cause for measurement errors !!!**

Application 1: OCT – Biometry - Optical Double-Beam Low Coherence Interferometry



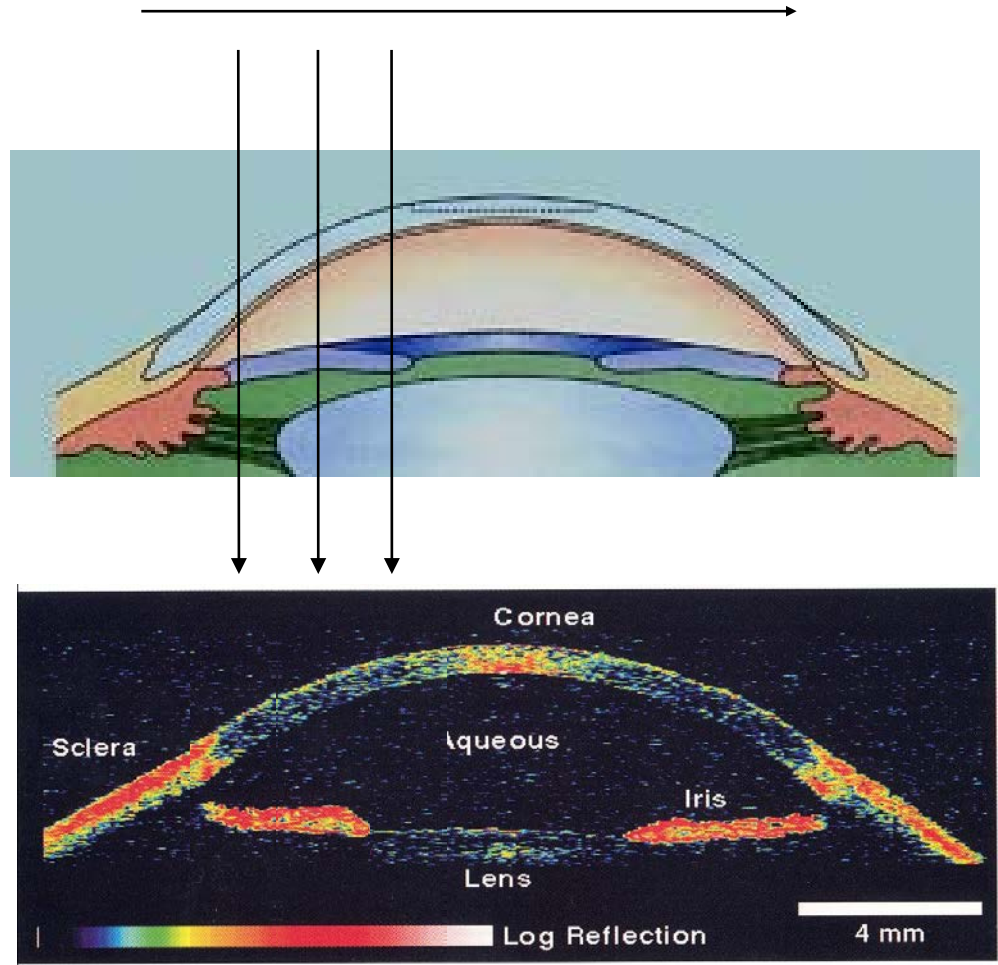
Application 1: OCT – Biometry - ZEISS IOLMaster



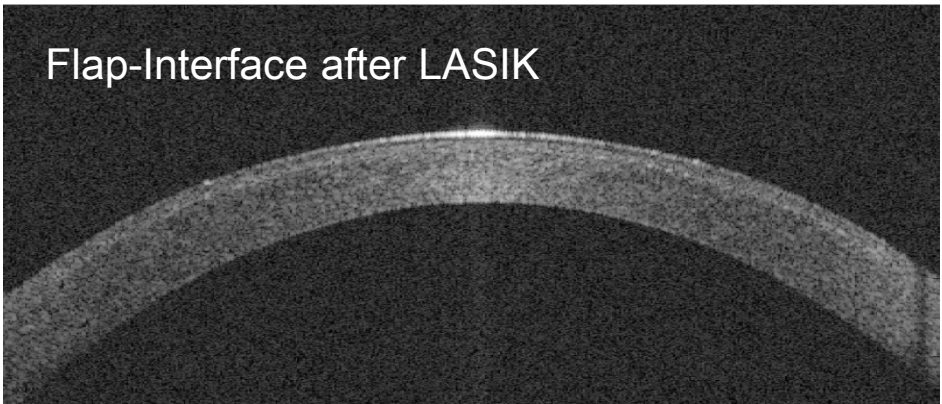
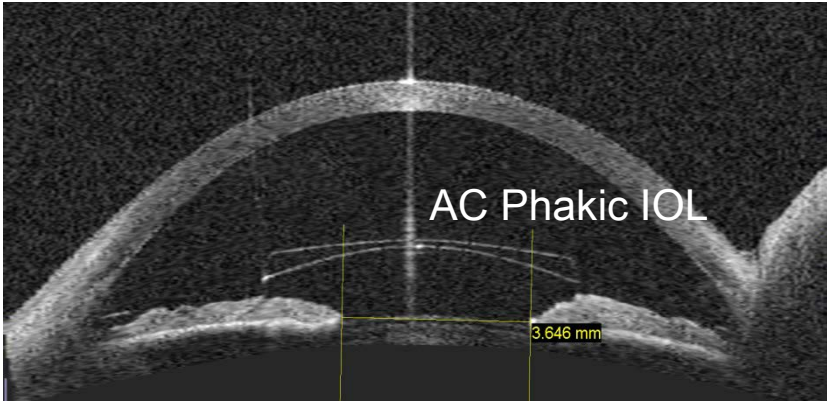
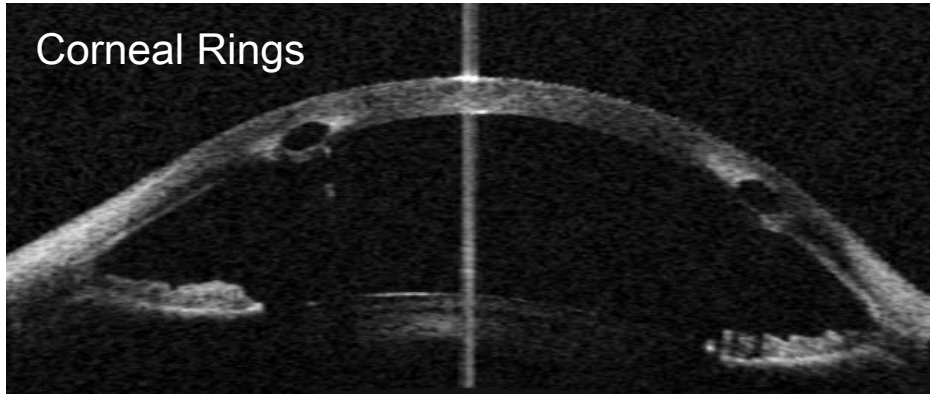
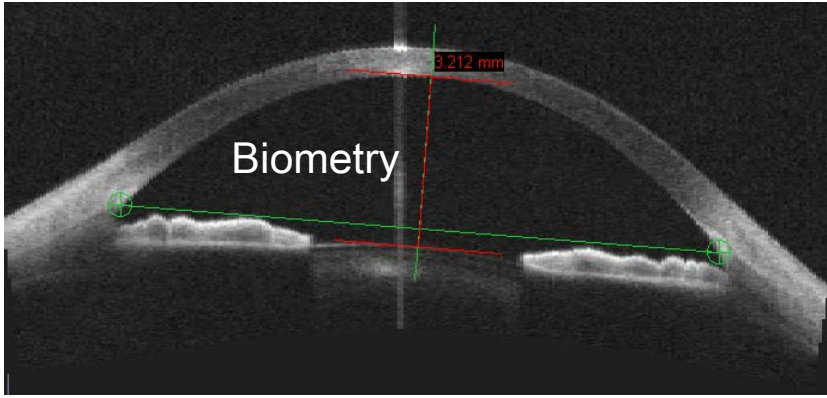
- 1. Non-invasive measurement**
no infection, no risk of injury,
no anesthesia necessary
- 2. Better post-operative results**
measurement along the visual axis,
no applanation, higher (5x) accuracy (30 μm)
- 3. Easy to use**
user independent, can be done by nurse
- 4. Time savings**

Application 2: Anterior Chamber Imaging

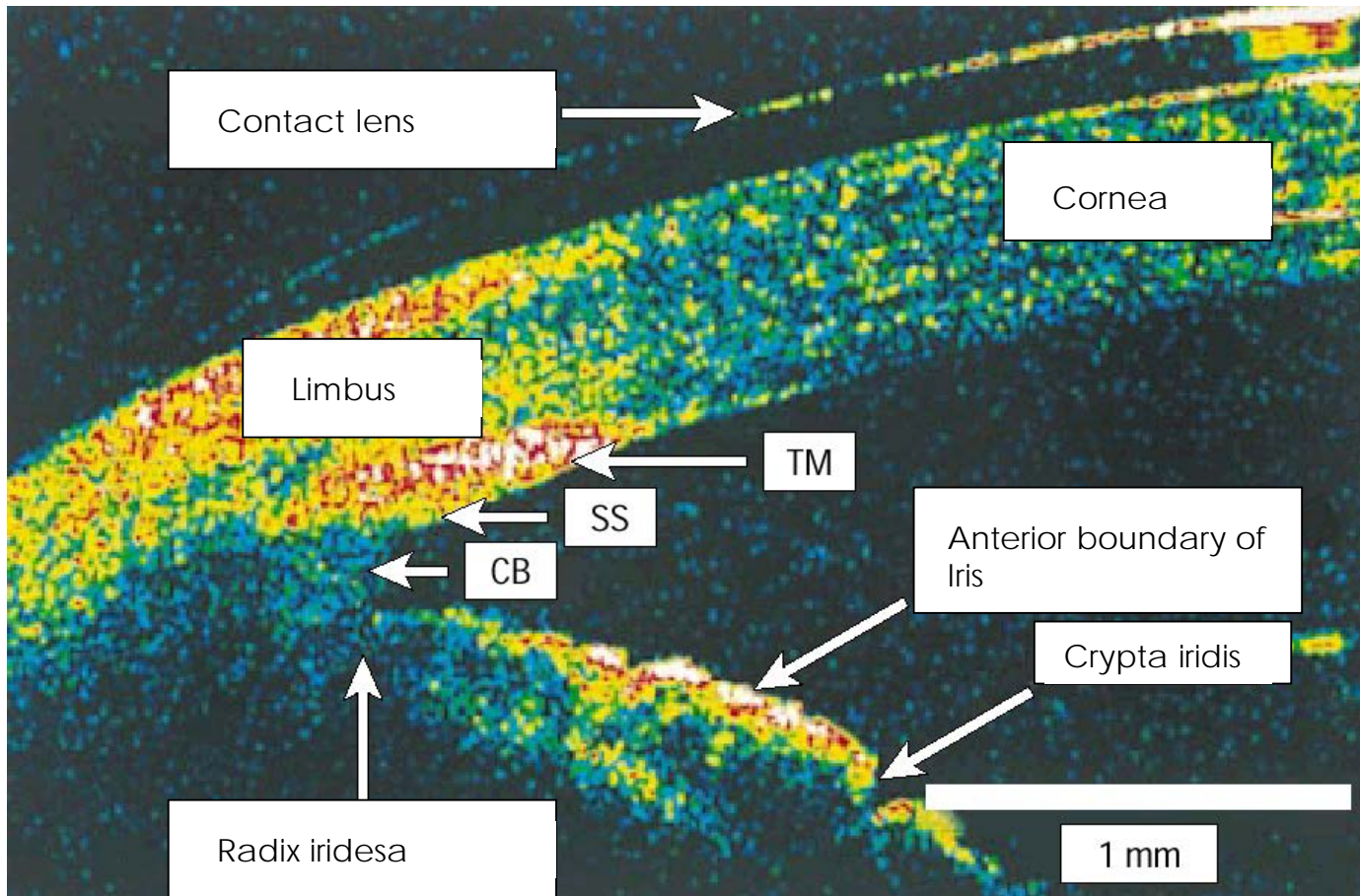
Transverse Scanning



Application 2: Anterior Chamber Imaging

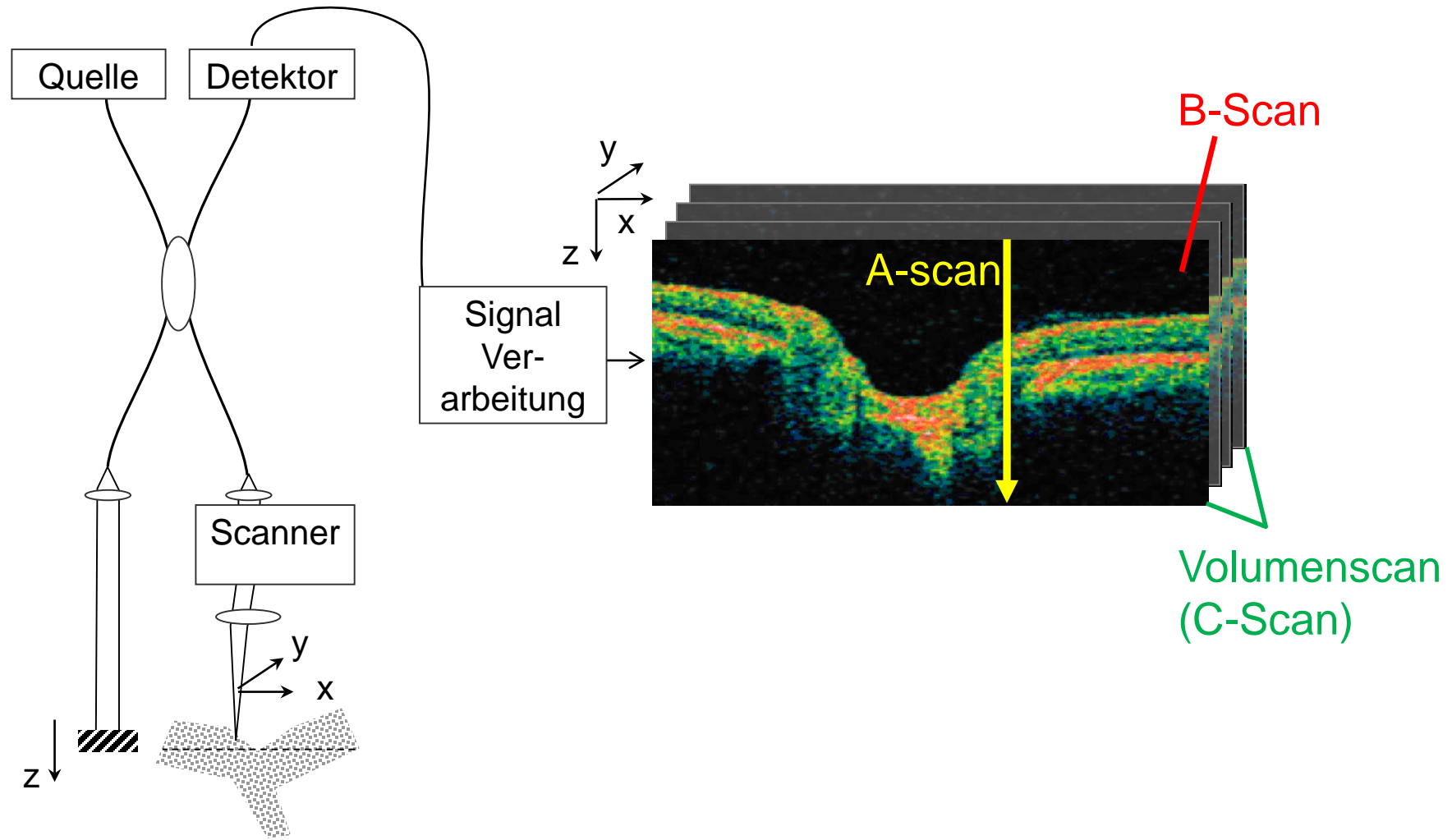


Application 2: Anterior Chamber Imaging



Detail Image of AC Chamber Angle

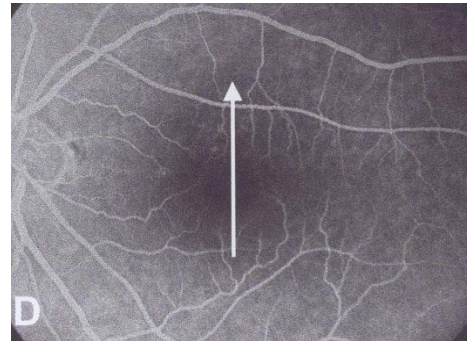
Application 3: Volume Scans of Retina



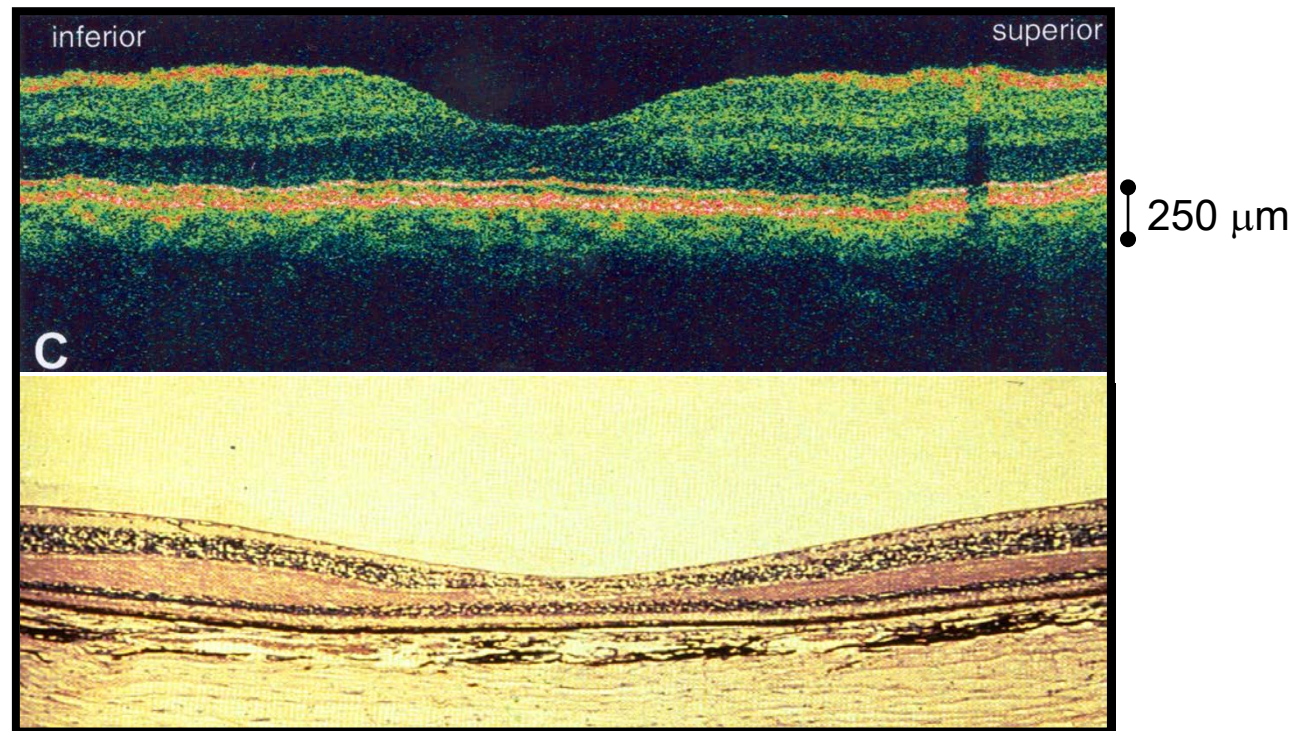
Application 3: Volume Scans of Retina

Fundus Image

OCT-Scan direction

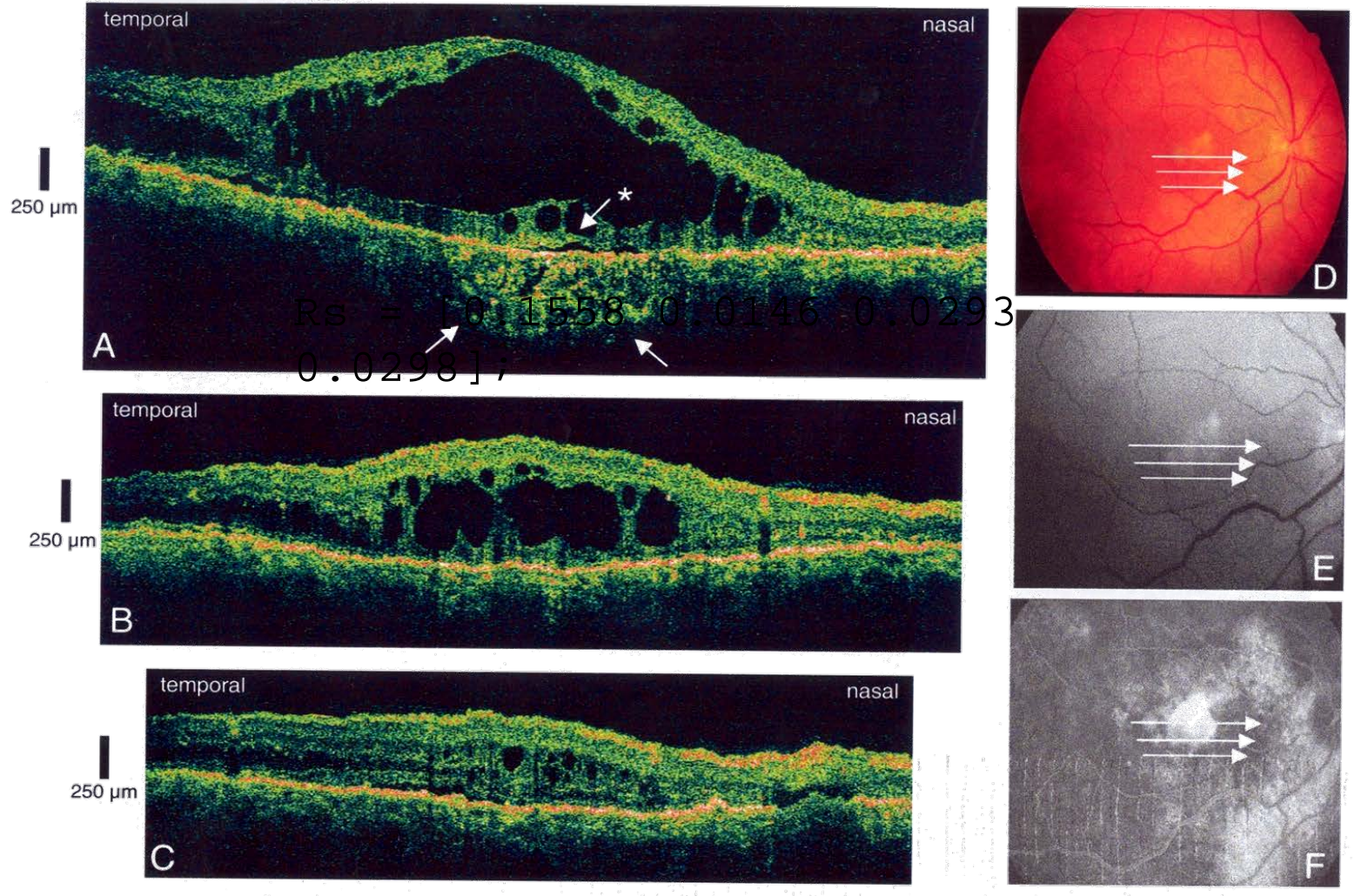


OCT
(non invasive)

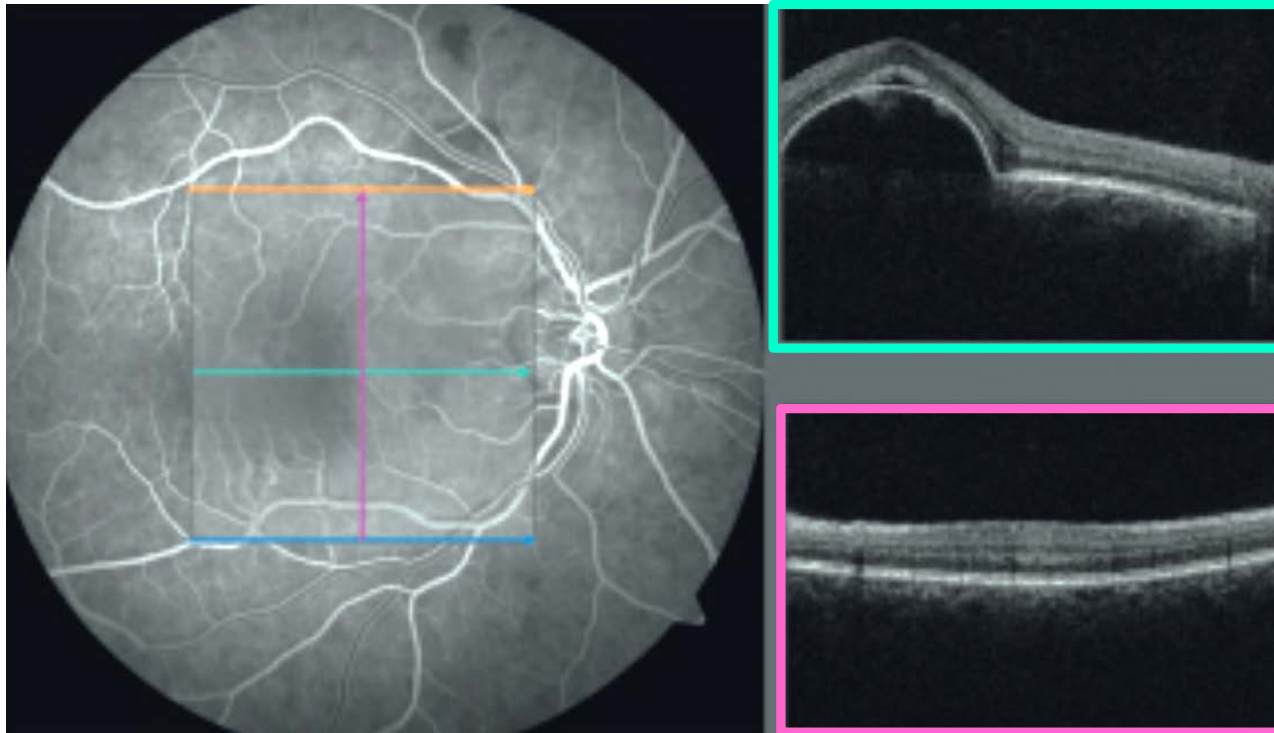


Histology

Application 3: Volume Scans of Retina - Edema



Application 3: Volume Scans of Retina – Retinal Detachment



Fundusbild
(Aufsicht)

OCT-Schnittbild
längs des Pfeiles

Application 4: Glaucoma-Diagnosis (Optic Nerve Head Analyse)

Optic Nerve Head Analysis

Individual Radial Scan Analysis

Rim Area (Vert. Cross Section):	1.107 mm ²
Avg Nerve Width @ Disk:	0.33 mm
Disk Diameter:	2.16 mm
Cup Diameter:	1.31 mm
Rim Length (Horiz.):	0.84 mm

Optic Nerve Head Analysis Results

Vert. Integrated Rim Area (Vol.)	0.217 mm ²
Horiz. Integrated Rim Width (Area)	1.767 mm ²
Disk Area	2.882 mm ²
Cup Area	1.637 mm ²
Rim Area	1.695 mm ²
Cup/Disk Area Ratio	0.401
Cup/Disk Horiz. Ratio	0.779
Cup/Disk Vert. Ratio	0.634

Personal

Name	Bauer Victor
BirthDate	05/04/1959

Scan

ScanType	Fast Optical Disk Analysis
ScanDate	10/09/2001
ScanLength	4.0

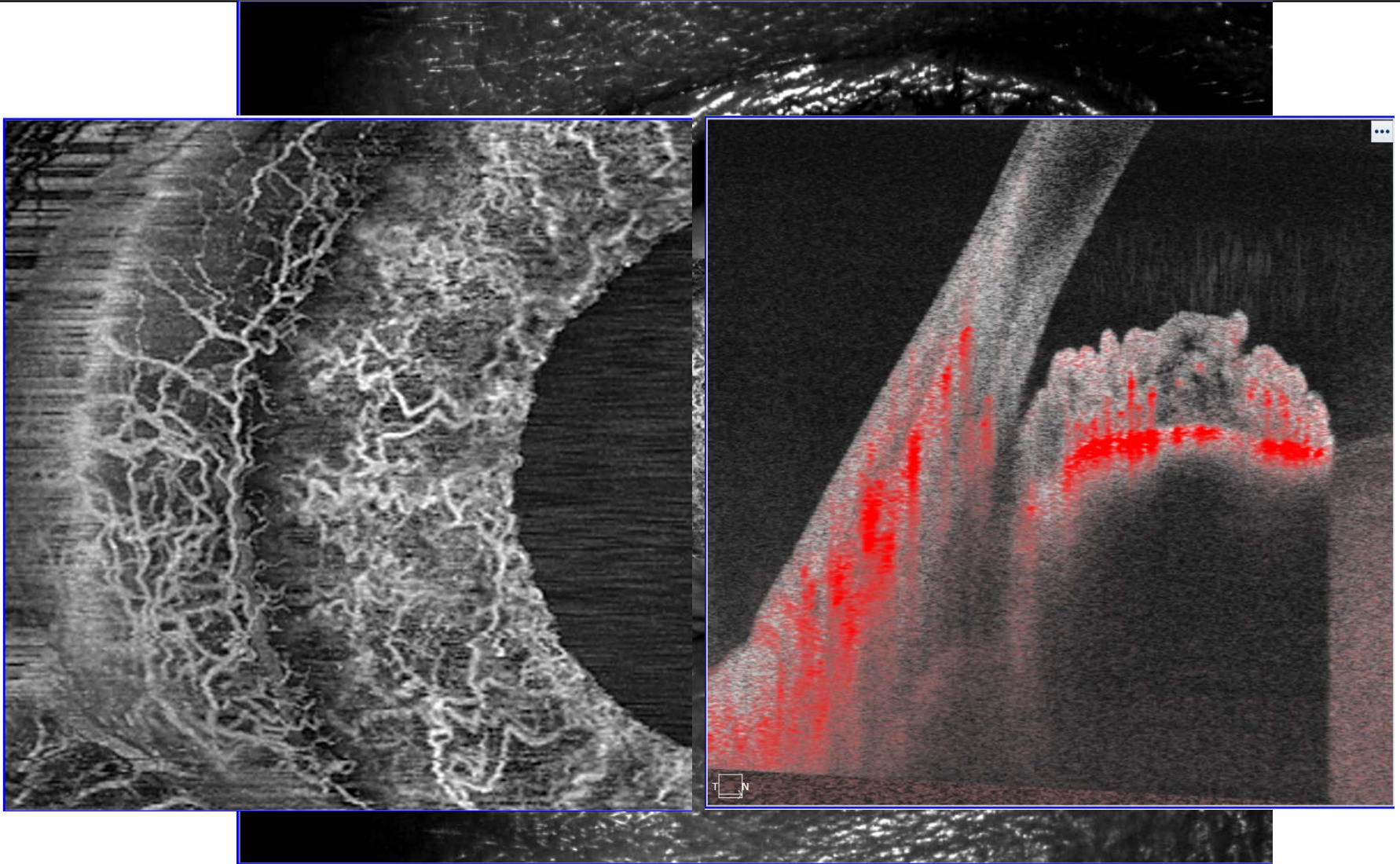
Plot Background: None Absolute Aligned and Shaded

Cup Offset for Topo (microns): 150

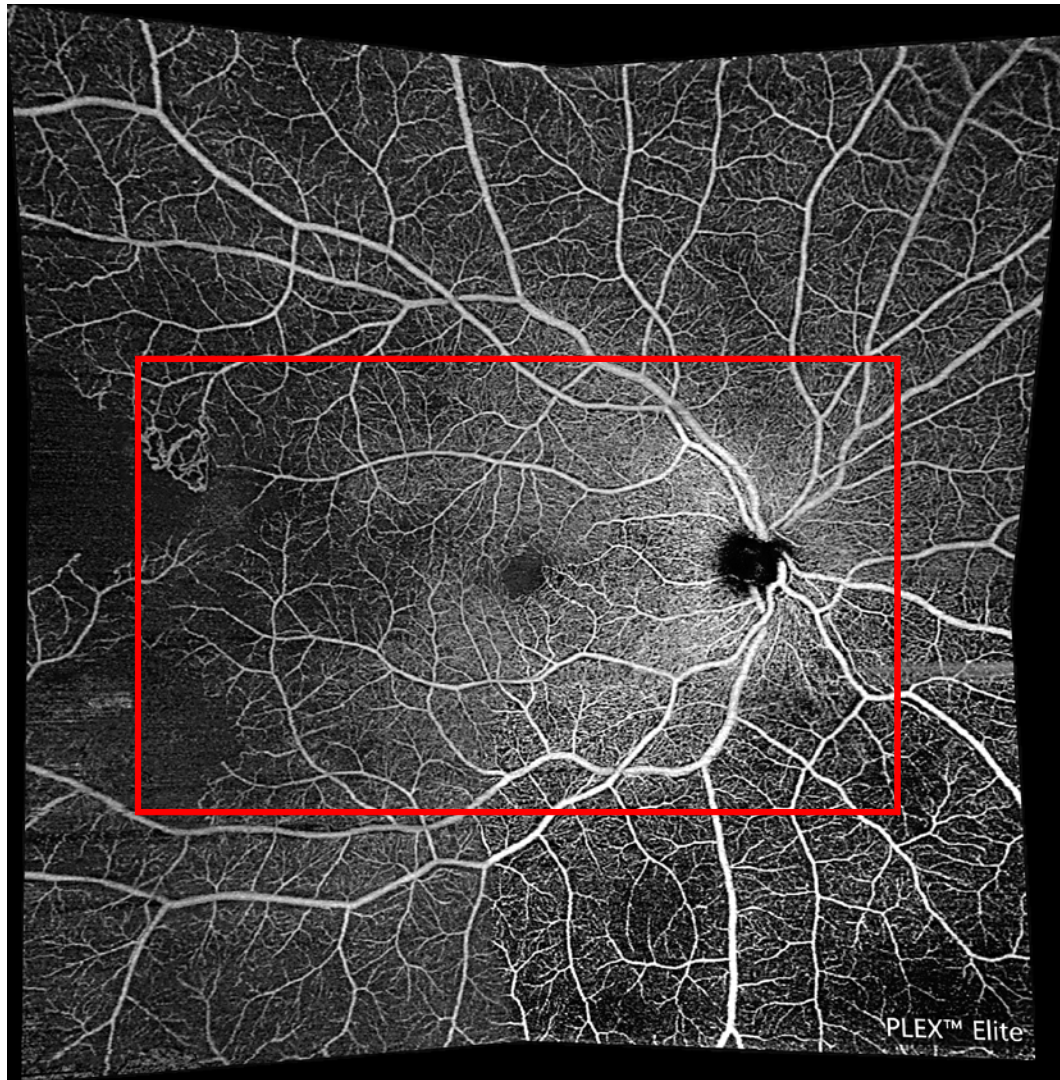
Cup Area (Topo): 1.329 mm²

Cup Volume (Topo): 0.28 mm³

Application 5: Angiography OCT – Anterior Segment OCT Angiography



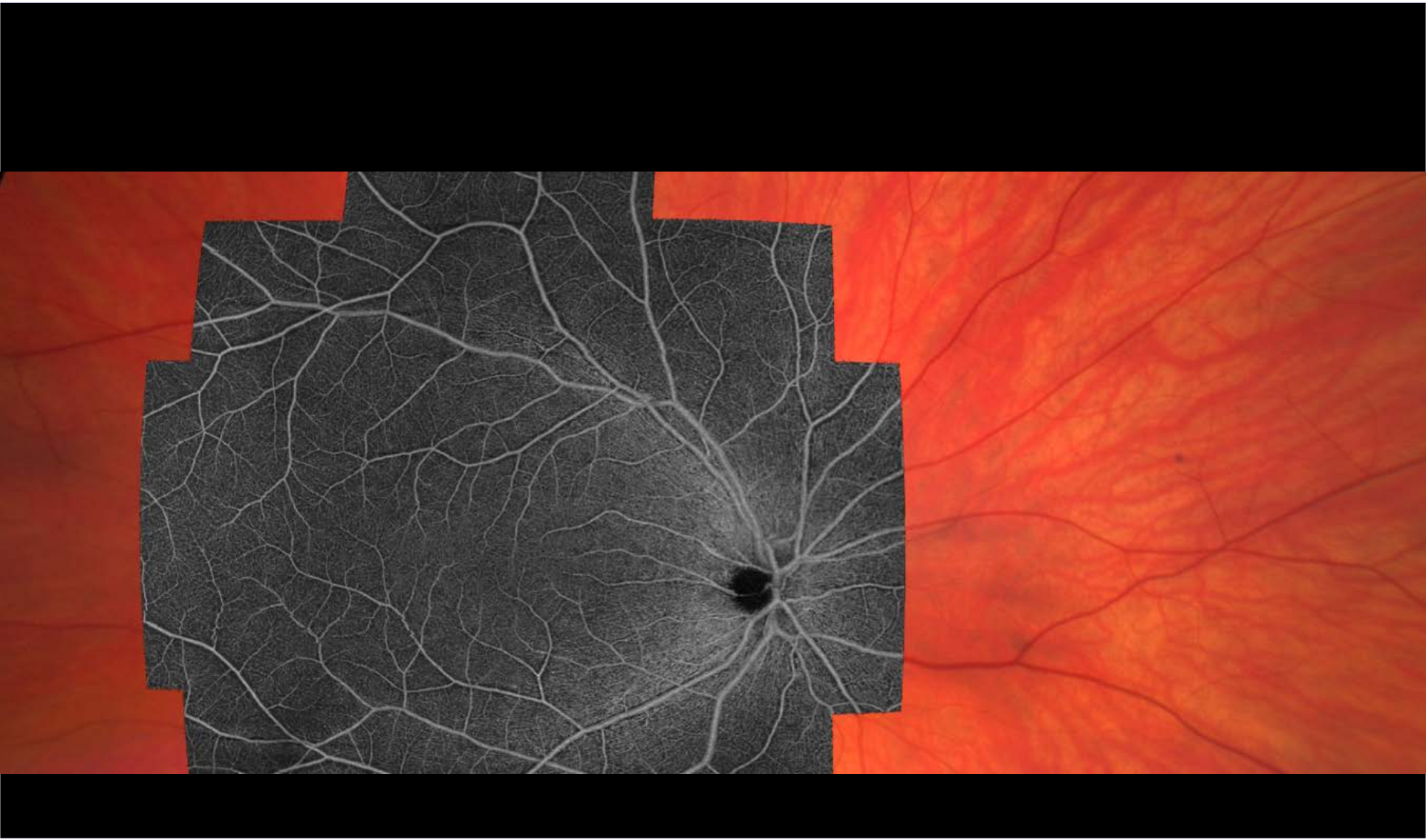
Application 5: Angiography OCT – Ultra-wide OCT Angiography Montage



Application 5: Angiography



Next generation Ultra-Widefield Fundus Imaging and CIRRUS OCT Angiography Montage



Next generation Ultra-Widefield Fundus Imaging

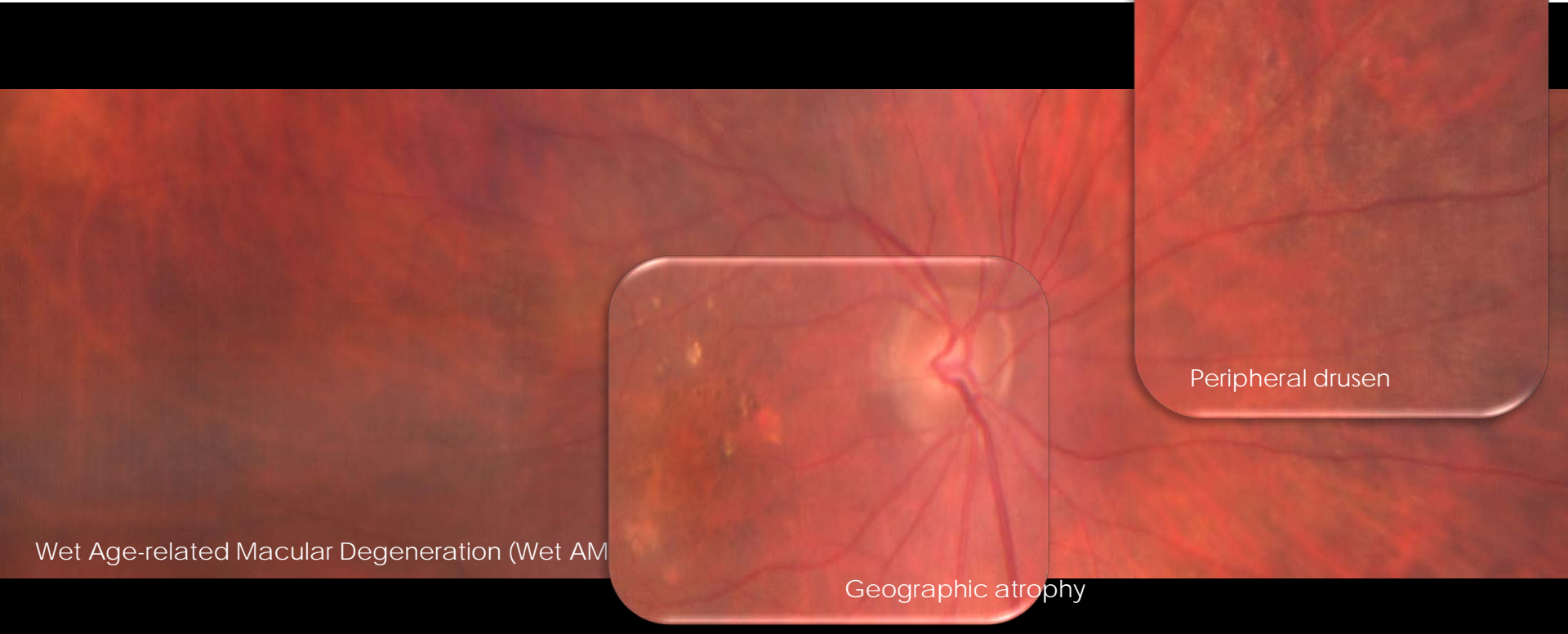


Image disease in the periphery with the color and clarity of a true color, high resolution traditional fundus camera